EPJ D
Atomic, Molecular, Optical and Plasma Physics
EPJ.org
your physics journal

Eur. Phys. J. D (2015) 69: 232 DOI: 10.1140/epjd/e2015-60319-9

Random unitary evolution model of quantum Darwinism with pure decoherence

Nenad Balanesković

edp sciences
Società Italiana di Fisica
Springer

Eur. Phys. J. D (2015) 69: 232
DOI: 10.1140/epjd/e2015-60319-9

THE EUROPEAN PHYSICAL JOURNAL D

Regular Article

Random unitary evolution model of quantum Darwinism with pure decoherence

Nenad Balaneskovića

Institut für Angewandte Physik, Technische Universität Darmstadt, 64289 Darmstadt, Germany

Received 29 May 2015 / Received in final form 15 August 2015
Published online 15 October 2015 – © EDP Sciences, Società Italiana di Fisica, Springer-Verlag 2015

Abstract. We study the behavior of Quantum Darwinism [W.H. Zurek, Nat. Phys. **5**, 181 (2009)] within the iterative, random unitary operations qubit-model of pure decoherence [J. Novotný, G. Alber, I. Jex, New J. Phys. **13**, 053052 (2011)]. We conclude that Quantum Darwinism, which describes the quantum mechanical evolution of an open system S from the point of view of its environment E, is not a generic phenomenon, but depends on the specific form of input states and on the type of S-E-interactions. Furthermore, we show that within the random unitary model the concept of Quantum Darwinism enables one to explicitly construct and specify artificial input states of environment E that allow to store information about an open system S of interest with maximal efficiency.

1 Introduction

From everyday-experience, classical states "pre-exist" objectively and as such constitute "classical reality" in a sense that the state of an open system S can be measured and agreed upon by many independent, mutually non-interacting observers, *without being disturbed*. This is done by intercepting fragments (≡observers) of the environment E (indirect or non-demolition measurement [1]). Thus, one may ask: *which sort of information about system S is* redundantly *and* robustly memorized by numerous distinct E-fragments, such that multiple observers may retrieve this same information in a non-demolishing fashion, thereby confirming the effective classicality of the S-state?

Zurek's concept of Quantum Darwinism tries to answer the above question by investigating what kind of information about system S the environment E can store and proliferate in a stable, complete and redundant way. It turns out that this redundantly stored information proliferated throughout environment E is the Shannon-entropy of the decohered system S, that contains information about S-pointer states [2,3].

These pointer-states, also known as interaction-robust S-states, are those S-states most immune (invariant) towards numerous interactions with the environment E. They are singled out by a characteristic dynamical phenomenon, an interaction-induced decoherence, which explains the process of destruction of quantum superpositions between states of an open quantum system S as a consequence of its interaction with an environment E. Most decoherence-based explanations of the emergence of classical S-states from quantum mechanical dynamics deal solely with observations which can be made at the level of system S, degrading its environment E to the role of a "sink" that carries away unimportant information about the preferred pointer-basis of the observed system S [1].

However, whereas the decoherence paradigm usually distinguishes between an open system S and its environment E, without specifying the structure of the latter, Quantum Darwinism subdivides the environment E into *non-overlapping subenvironments* (fragments or "storage cells") accessible to measurements, that have already interacted with system S in the past and thus enclose Shannon-information (entropy) about its preferred (pointer) states (i.e. E-registry states are assumed to have a *tensor product* structure). In other words, Quantum Darwinism changes the perspective and regards the environment E as a large resource ("quantum memory") which could be used for indirect acquisition and storage of relevant information about system S and its pointer-basis (i.e. E becomes a "witness" to the observed S-state) [3].

Accordingly, one can quantify the "degree of objectivity" of S-states by simply counting the number of copies of their information record in environment E. This number of copies of the information deposited by a particular S-state into environmental fragments after many S-E-interactions reveals its redundancy R. The higher the R of a particular S-state, the more "classical" it appears.

Similar to the Darwinistic concept "survival of the fittest", the S-pointer states represent the "fittest" ("quasi-classical") states of an open system S that survive numerous S-E-interactions (measurements) long enough to deposit (imprint) multiple copies of their information into environment E [4]. Ergo: high information redundancy of S-states within environment E implies that information about the "fittest" observable (pointer state) of

a e-mail: balaneskovic@gmx.net

system S that survived constant monitoring by the environment E has been successfully distributed throughout all E-fragments, enabling the environment to store redundant copies of information about preferred S-observables and thus account for their objective existence ("einselection" [5,6]).

In the following we intend to compare two qubit models of Quantum Darwinism: Zurek's C(ontrolled-)NOT-evolution model [3] and the random unitary operations model [7–9] of an open k-qubit system S interacting with an n-qubit environment E. According to Zurek's qubit model the one qubit ($k = 1$) open system S acts via CNOT-transformations as a control unit upon each of the n mutually non-interacting E-qubits (targets) *only once*. On the other hand, the random unitary evolution generalizes Zurek's interaction procedure by iterating the directed graph (digraph) of CNOT-interactions between a $k \geq 1$ qubit system S and mutually non-interacting E-qubits, represented by the corresponding quantum operation channel, $N \gg 1$ times until the underlying dynamics forces the input state $\hat{\rho}_{SE}^{in}$ of the entire system to converge to the output state $\hat{\rho}_{SE}^{out}$. Such asymptotically evolved $\hat{\rho}_{SE}^{out}$ can then be described by a subset of the total Hilbert-space $\mathcal{H}_{SE} = \mathcal{H}_S \otimes \mathcal{H}_E$, the so-called *attractor space*, and attractor states therein.

From the practical point of view, we want to answer two questions. First: which $\hat{\rho}_{SE}^{in}$ lead to Quantum Darwinism? Second: does Quantum Darwinism, and thus a perfect transfer of Shannon-entropy into environment E, depend on a specific model being used, or is it a model-independent phenomenon? Namely, since the random unitary evolution can model systems S subject to pure decoherence by singling out the corresponding pointer states as a result of the asymptotic iterative dynamics, it also enables one to specify (in comparison with Zurek's model) which types of input states $\hat{\rho}_{SE}^{in}$ store the "classical" Shannon information about system S and its pointer-basis efficiently into environment E. Finally, we also want to use the random unitary model to see whether Quantum Darwinism appears if we introduce into the corresponding interaction digraph CNOT-interactions between E-qubits.

This article is organized as follows: Section 2 deals with basic physical and mathematical concepts of Quantum Darwinism (mutual information, CNOT transformation, partial information plots, S-pointer states) and discusses this phenomenon within the framework of Zurek's qubit CNOT-evolution toy model [3]. We thereby see that for an open pure k-qubit S-input state $\hat{\rho}_S^{in}$ the CNOT transformation leads to Quantum Darwinism only if one starts with $\hat{\rho}_{SE}^{in} = \hat{\rho}_S^{in} \otimes \hat{\rho}_E^{in}$ and $\hat{\rho}_E^{in}$ prepared as a pure n-qubit E-registry state. In Section 3 we first introduce the mathematical formalism of iterated random unitary evolution [7–9]. In Sections 3.1 and 3.4 we show that introducing CNOT-interactions between E-qubits suppresses the appearence of Quantum Darwinism. In Section 3.2 we present numerical results of the iterated random unitary evolution, concluding that Zurek's qubit model of Quantum Darwinism cannot be interpreted as a short-time limit ($\equiv$small number N of iterations) of the random unitary evolution model.

Then we turn our attention in Section 3.3 to the asymptotic ($N \gg 1$) behavior of mutual information within the random unitary qubit model. This asymptotic behavior of mutual information of iterated, random unitarily evolved output states $\hat{\rho}_{SE}^{out}$ allows us to conclude that Quantum Darwinism and its appearence depends in general on an underlying model used to describe interactions between S- and E-qubits. Finally, we summarize the most important results of our discussion before giving a brief outlook on interesting future research problems connected with Quantum Darwinism (Sect. 4). All detailed analytic calculations are given in 4 appendices: Appendix A displays output states $\hat{\rho}_{SE}^{out}$ of Zurek's CNOT-evolution used in Section 2. Appendix B explains why only the CNOT-transformation leads to Quantum Darwinism, both in Zurek's and the random unitary evolution model. In Appendix C we derive (dimensionally) maximal and minimal attractor subspaces that are used in the course of interpretation of random unitarlly evolved $\hat{\rho}_{SE}^{out}$ in Section 3. Finally, Appendix D contains a list of $\hat{\rho}_{SE}^{out}$ obtained by means of (dimensionally) maximal and minimal attractor spaces that are necessary for the discussion of the random unitary evolution in Section 3.

2 A qubit toy-model of quantum Darwinism

In this section we briefly describe the simplest qubit model of Quantum Darwinism, as suggested by Zurek [3], involving an open pure $k = 1$-qubit S (given by the state vector $|\Psi_S^{in}\rangle = a|0\rangle + b|1\rangle$, $(a, b) \in \mathbb{C}$ in the standard computational basis, where $|a|^2 + |b|^2 \stackrel{!}{=} 1$), which acts as a control-unit on its ($n \in \mathbb{N}$)-qubit target (environment) $E \equiv \mathcal{E}_1 \otimes \mathcal{E}_2 \otimes \ldots \otimes \mathcal{E}_n$.

Subsequently, we apply Zurek's qubit evolution model to different input states $\hat{\rho}_{SE}^{in}$ of the total system and investigate whether Quantum Darwinism appears within this model with respect to different members of a one-parameter family of unitary transformations that also encloses, as a special case, the unitary C(ontrolled)-NOT operation. According to Zurek's qubit model the interaction between system S and environment E has to occur as follows:

1. Start with a pure $k = 1$-qubit open $\hat{\rho}_S^{in} = |\Psi_S^{in}\rangle\langle\Psi_S^{in}|$ and an arbitrary n-qubit $\hat{\rho}_E^{in}$, where $\hat{\rho}_{SE}^{in} = \hat{\rho}_S^{in} \otimes \hat{\rho}_E^{in}$.
2. Apply the CNOT-gate $\hat{U}_{CNOT}|i\rangle_S|j\rangle_E = |i\rangle_S|i \oplus j\rangle_E$ (where $\oplus$ denotes addition modulo 2), such that the S-qubit$i$ interacts successively and only once with each qubit j of E until all n E-qubits have interacted with S, resulting in an entangled state $\hat{\rho}_{SE}^{out}$.
3. Trace out successively (for example from *right to left*) $(n-L)$ qubits in $\hat{\rho}_E^{out}$ and $\hat{\rho}_{SE}^{out}$ – this yields the L-qubit $\hat{\rho}_{E_L}^{out}$ and $\hat{\rho}_{SE_L}^{out}$, with $0 < L \leq n$, and an environmental fraction parameter $0 < f = \frac{L}{n} \leq 1$.
4. Compute the eigenvalue spectra $\{\lambda_1, \ldots, \lambda_{d(f)}\}$ of $\hat{\rho}_S^{out}$, $\hat{\rho}_{E_f}^{out}$ and $\hat{\rho}_{SE_f}^{out}$ and the f-dependent von Neumann

entropies

$$H\left(\hat{\rho}\left(f\right)\right) = -\sum_{i=1}^{d(f)} \lambda_i \log_2 \lambda_i \geq 0, \sum_{i=1}^{d(f)} \lambda_i \stackrel{!}{=} 1$$

(where $d(f)$ is the dimensionality of $\hat{\rho}(f)$ in question).

5. Divide all entropies by $H(S_{class})$ to obtain the ratio $I(S:E_f)/H(S_{class})$ depending on the E-fraction parameter f, with **mutual information** (MI)

$$I\left(S:E_f\right) = H\left(S\right) + H\left(E_f\right) - H\left(S,E_f\right), \quad (1)$$

that quantifies the amount of the proliferated Shannon entropy ("classical information") [4,10]

$$H\left(S_{class}\right) = -\sum_i p_i \log_2 p_i = H\left(\{|\pi_i\rangle\}\right), \quad (2)$$

where probabilities $p_i = \mathbf{Tr}_E\langle\pi_i|\hat{\rho}_{SE}^{class}|\pi_i\rangle$ emerge as partial traces of an effectively decohered ("quasi classical") S-state $\hat{\rho}_S^{class}$ w.r.t. the particular S-pointer-basis $\{|\pi_i\rangle\}$, and the redundancy

$$\begin{gathered} R = 1/f^* \ (0 < f^* \leq 1) \\ \text{with } I\left(S:E_{f=f^*}\right) \approx H\left(S_{class}\right) (n \gg 1) \end{gathered} \quad (3)$$

of the measured $\{|\pi_i\rangle\}$ in the limit $n \gg 1$ of effective decoherence.

6. Finally, plot $I(S:E_f)/H(S_{class})$ vs. $0 < f \leq 1$ (Partial Information Plot (PIP) of MI).

Now we look at the specific input state

$$\hat{\rho}_{SE}^{in} = \left|\Psi_S^{in}\right\rangle\left\langle\Psi_S^{in}\right| \otimes |0_n\rangle\langle 0_n|$$

with $|0_n\rangle \equiv |0\rangle^{\otimes n}$ (ground state $\hat{\rho}_E^{in}$) [3]. Let the one S-qubit transform each E-qubit via CNOT *only once* until the entire environment E is affected, giving $\forall L > 0$

$$\left|\Psi_{SE_{L=n}}^{out}\right\rangle = a\,|0\rangle \otimes |0_{L=n}\rangle + b\,|1\rangle \otimes |1_{L=n}\rangle, \quad (4)$$

with von Neumann-entropies

$$\begin{aligned} H\left(S,E_L\right) &= H\left(S_{class}\right)\cdot\left(1-\delta_{L,n}\right) \\ H\left(E_L\right) &= H\left(S\right) = H\left(S_{class}\right) \\ H\left(S_{class}\right) &= -|a|^2\log_2|a|^2 - |b|^2\log_2|b|^2. \end{aligned}$$

Equation (4) shows that $I\left(S:E_f\right)$, after the Lth E-qubit has been taken into account, increases from zero to the value

$$I\left(S:E_f\right) \equiv H\left(S_{class}\right) \Rightarrow I\left(S:E_f\right)/H\left(S_{class}\right) = 1,$$

implying that each fragment (qubit) of environment E supplies complete information about the S-pointer observables $\{|\pi_i\rangle\}$. Since the very first CNOT-operation forces the system S to decohere completely into its pointer basis $\{|\pi_i\rangle\} \equiv \{|0\rangle, |1\rangle\}$, one encounters the influence of Quantum Darwinism on system S: from all possible S-states, which started its dynamics within a pure $\hat{\rho}_S^{in}$, only diagonal elements survive constant monitoring of environment E, whereas off-diagonal elements of $\hat{\rho}_S^{in}$ vanish due to decoherence, i.e. monitoring of system S by its environment E selects a preferred $\{|\pi_i\rangle\}$, leading to a continued increase of its R throughout the environment E.

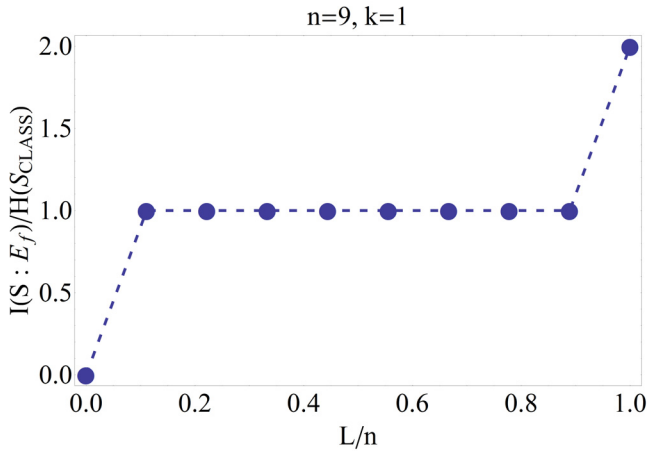

Fig. 1. PIP of MI and R of $H(\hat{\rho}_S^{out}) = H(S_{class})$ stored in E w.r.t. $0 < f = L/n \leq 1$, $k = 1$ qubit pure $\hat{\rho}_S^{in}$, $\hat{\rho}_E^{in} = |0_n\rangle\langle 0_n|$, $\hat{\rho}_{SE}^{in} = \hat{\rho}_S^{in} \otimes \hat{\rho}_E^{in}$ in (4), after $\hat{U}_{\text{CNOT}}$-evolution in accord with Zurek's model [3].

After decoherence we obtain

$$I\left(S:E_f\right) = H\left(S_{class}\right) = H\left(E_f\right) = H\left(S,E_f\right),$$

valid for any E-fragment, as long $f < 1$. After inclusion of the entire environment E ($f = 1$) we obtain the maximum

$$I\left(S:E\right) = 2H\left(S_{class}\right)$$

of MI ("quantum peak", accessible through global measurements of $\hat{\rho}_{S,E}^{out}$ due to $H(S,E_{f=1}) = 0$). Since each E-qubit in equation (4) is assumed to contain a perfect information replica about $\{|\pi_i\rangle\}$, its R is given by the number of qubits in the environment E, e.g. $R = n$. This constrains the form of MI in its PIP (see Fig. 1), which jumps from 0 to $H(S_{class})$ of S at $f = f^* = 1/n$, continues along the "plateau" until $f = 1 - 1/n$, before it eventually jumps up again to $2H(S_{class})$ at $f = 1$.

$I(S:E_f)/H(S_{class}) \geq 1$ indicates high R (objectivity) of $H(S_{class})$ proliferated throughout E. Also, by intercepting already one E-qubit we can reconstruct $\{|\pi_i\rangle\}$, regardless of the order in which the n E-qubits are being successively traced out. Only if we need a small fraction of the environment E enclosing maximally $n \cdot f^* = k \ll n$ E-qubits [3], to reconstruct $\{|\pi_i\rangle\}$, Quantum Darwinism appears: i.e., it is not only important that the PIP-'plateau' appears, more relevant is its length $1/f^* \equiv R$ of $\{|\pi_i\rangle\}$. The main question we aim to address w.r.t. Zurek's and the random unitary operations model is: which types of input states $\hat{\rho}_{SE}^{in}$ validate the relation

$$\frac{I\left(S:E_f\right)}{H\left(S_{class}\right)} = \frac{H\left(S\right) + H\left(E_f\right) - H\left(S,E_f\right)}{H\left(S_{class}\right)} \geq 1, \quad (5)$$

with $H(S) \approx H(S_{class})$ and $H(E_f) \geq H(S,E_f)$ at least for all $(k \leq L \leq [n \gg 1])$, regardless of the order in which

the n E-qubits are being successively traced out from the output state $\hat{\rho}_{SE}^{out}$? In order to answer this question we discuss in the following the f-dependence of MI for different $\hat{\rho}_{SE}^{in}$ from the point of view of Zurek's qubit model. Figure 2 below displays the behavior of the MI vs f for different $\hat{\rho}_{E}^{in}$ from Table A.1 in Appendix A which justifies the following conclusions:

It is in general important in which order one traces out E-qubits from the output-state $\hat{\rho}_{SE_L}^{out}$, as indicated by the •-dotted curve (Quantum Darwinism appears) and the ■-dotted curve (no Quantum Darwinism, since the relation $H(E_L) = H(S, E_L)$ holds only $\forall(k < L \leq n)$, but not for $L = k$) in Figure 2: when tracing out E-qubits as in equation (4) from right to Quantum Darwinism appears only if, for each fixed value of $(k \leq L < n)$, $\hat{\rho}_{SE_L}^{out}$ acquires the structure displayed in equation (4), that emerges when starting the CNOT-evolution with a pure, n-qubit registry input state of the environment $\hat{\rho}_{E}^{in} = |0_n\rangle\langle 0_n|$.

Introducing classical correlations into $\hat{\rho}_{SE}^{in} = \hat{\rho}_{S}^{in} \otimes \hat{\rho}_{E}^{in}$ (with a one-qubit pure $\hat{\rho}_{S}^{in}$) by writing $\hat{\rho}_{E}^{in}$ as a convex sum of pure n-qubit registry states $\{|y\rangle\langle y|, y \in \{0, \ldots, 2^n - 1\}\}$ (rank one operators) in the standard computational basis tends in general to suppress the appearance of the MI-plateau: in case of a totally mixed $\hat{\rho}_{E}^{in}$ the MI is even zero $\forall(0 < L < n)$, as indicated by the ♦-dotted and ▲-dotted curves in Figure 2. Quantum correlations within $\hat{\rho}_{E}^{in}$ do not improve the situation, but lead in general to the relation $H(S) = H(\hat{\rho}_{S}^{out}) < H(S_{class})$ instead, as shown by the ▼-dotted curve in Figure 2.

We can extend Zurek's interaction algorithm to systems S with more than one qubit $(k > 1)$ by assuming the environment E to contain $n' = kn \gg k$ qubit-cells (i.e. one subdivides n' E-qubits into k disjoint subsets $E \equiv \bigcup_{i=1}^{k} E_i$ with $|E_i| = n\,\forall i$) and allowing each S-qubit to interact with only one E_i-subset of environment E and only once with each of the $n \gg k$ E-qubits within the particular E_i.

Then, with $\hat{\rho}_{SE}^{in} = \hat{\rho}_{S}^{in} \otimes \hat{\rho}_{E}^{in}$, for $\hat{\rho}_{E}^{in} = |0_{n'}\rangle\langle 0_{n'}|$ and a pure two-qubit $(k = 2)$ state $\hat{\rho}_{S}^{in}$, the corresponding PIP is given for all $(k = 2 \leq L \leq n' - k)$ by the •-dotted plateau in Figure 2, whereas[1]

$$H(S, E_L) < H(E_L), \quad n' - k + 1 \leq L \leq n'$$
$$0 \leq I(S : E_{L=1}) / H(S_{class}) \leq 0.5, \quad 0 < L < k = 2.$$

Thus, in Zurek's pure decoherence qubit-model of Quantum Darwinism the specified CNOT-evolution yields the MI-plateau also for pure $\hat{\rho}_{S}^{in}$ with $k > 1$ qubits if we start its evolution within $\hat{\rho}_{SE}^{in} = \hat{\rho}_{S}^{in} \otimes \hat{\rho}_{E}^{in}$ and with a pure one registry n'-qubit state $\hat{\rho}_{E}^{in} = |y\rangle\langle y|$ in the standard computational basis $(y \in \{0, \ldots, 2^{n'} - 1\})$.

Certainly, if we deliberately design $\hat{\rho}_{SE}^{in}$ such that it remains unaltered under the CNOT-evolution by entangling the pointer-basis $\{|\pi_i\rangle\} \equiv \{|0\rangle, |1\rangle\}$ of a $k = 1$ qubit system S with one-qubit E-eigenstates $|s_1\rangle = 2^{-1/2}(|0\rangle + |1\rangle)$ and $|s_2\rangle = 2^{-1/2}(|0\rangle - |1\rangle)$ of the CNOT-transformation (Pauli matrix) $\hat{\sigma}_x$ according to

$$\left|\Psi_{SE}^{in}(L = n)\right\rangle = a\,|0\rangle \otimes \left|s_1^{L=n}\right\rangle + b\,|1\rangle \otimes \left|s_2^{L=n}\right\rangle$$
$$\left|s_m^L\right\rangle = |s_m\rangle^{\otimes L},\ \hat{\sigma}_x\,|s_m\rangle = \underbrace{(-1)^{m+1}}_{:=\lambda}|s_m\rangle \qquad (6)$$

(with $m \in \{1, 2\}$, $\langle s_1|s_2\rangle = 0$), (6) would lead to the PIP displayed in Figure 1: i.e. Quantum Darwinism would appear. One can even show that (6) leads to Quantum Darwinism only for $k = 1$ qubit system S (see. Appendix B).

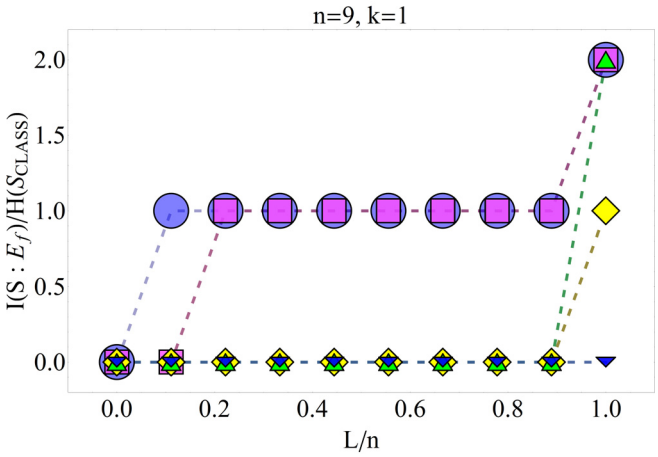

Fig. 2. PIP for $\hat{\rho}_{SE}^{out}$ from $\hat{\rho}_{SE}^{in} = |\Psi_S^{in}\rangle\langle\Psi_S^{in}| \otimes \hat{\rho}_{E}^{in}$ (where $k = 1$, $n = 9$, $|\Psi_S^{in}\rangle = a|0\rangle + b|1\rangle$) and different $\hat{\rho}_{E}^{in}$ (see. also Tab. A.1 in Appendix A) in Zurek's qubit model.

3 Random unitary model of quantum Darwinism

In the present section we summarize the iterative evolution formalism of the random unitary model before discussing its most important results regarding Quantum Darwinism in Sections 3.1–3.4.

Random unitary operations can model the pure decoherence of open system S with k qubits (control, index i) interacting with n E-qubits (targets j) (as indicated in the directed interaction graph (digraph) in Fig. 3) by the one-parameter family of two-qubit "controlled-U" unitary transformations (in the standard one-qubit computational basis $\{|0\rangle, |1\rangle\}$)

$$\widehat{U}_{ij}^{(\phi)} = |0\rangle_i\langle 0| \otimes \widehat{I}_1^{(j)} + |1\rangle_i\langle 1| \otimes \widehat{u}_j^{(\phi)} \qquad (7)$$

(where $\widehat{I}_1^{(j)} = |0\rangle_j\langle 0| + |1\rangle_j\langle 1|$). Equation (7) indicates that only if an S-qubit i should be in an excited state, the corresponding targeted E-qubit j hast to be modified by a $(0 \leq \phi \leq \pi)$-parameter $\widehat{u}_j^{(\phi)}$ [8] (with Pauli matrices $\hat{\sigma}_l$, $l \in \{x, y, z\}$)

$$\widehat{u}_j^{(\phi)} = \hat{\sigma}_z^{(j)} \cos\phi + \hat{\sigma}_x^{(j)} \sin\phi \Rightarrow \widehat{u}_j^{(\phi=\pi/2)} = \hat{\sigma}_x^{(j)}, \qquad (8)$$

[1] The lower bound follows from the trivial initial probability distribution$\{|a_i|^2 = 1, |a_{i'}|^2 = 0\,\forall i' \neq i\}$, whereas the upper bound emerges from $\{|a_i|^2 = 2^{-k}\}_{i=0}^{2^k-1}\forall i$ in $\hat{\rho}_{S}^{in}$.

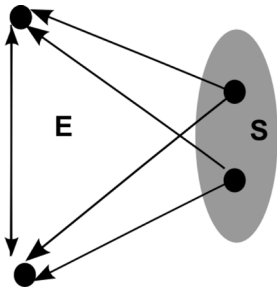

Fig. 3. Interaction digraph (ID) between system S and environment E with pure decoherence within the random unitary model [8].

which for $\phi = \pi/2$ yields the CNOT-gate [7–9]. Arrows of the interaction digraph (ID) in Figure 3 from S- to E-qubits represent two-qubit interactions $\widehat{u}_j^{(\phi)}$ between randomly chosen qubits i and j with probability distribution p_e used to weight the edges $e = (ij) \in M$ of the digraph (E-qubits are in general allowed to interact among themselves).

All interactions are well separated in time. The S-qubits do not interact among themselves. In order to model the decoherence-induced measurement process of system S by environment E we let an input state $\hat{\rho}_{SE}^{in}$ evolve by virtue of the following iteratively applied random unitary quantum operation (completely positive unital map) $\mathcal{P}(.) \equiv \sum_{e\in M} K_e(.)K_e^\dagger$ (with Kraus-operators given by $K_e := \sqrt{p_e}\widehat{U}_e^{(\phi)}$) [7–9]:

1. The quantum state $\hat{\rho}(N)$ after N iterations is changed by the $(N+1)$th iteration to the quantum state (quantum Markov chain)

$$\widehat{\rho}\,(N+1) = \sum_{e\in M} p_e \widehat{U}_e^{(\phi)} \widehat{\rho}\,(N)\, \widehat{U}_e^{(\phi)\dagger} \equiv \mathcal{P}\left(\widehat{\rho}\,(N)\right). \quad (9)$$

2. In the asymptotic limit $N \gg 1$ $\widehat{\rho}(N)$ is independent of $(p_e,\, e \in M)$ and determined by linear attractor spaces $\mathcal{A}_\lambda \subset \mathcal{H}_{SE}$, as subspaces of the total S-E-Hilbert space $\mathcal{H}_{SE} = \mathcal{H}_S \otimes \mathcal{H}_E$ to the eigenvalues λ (with $|\lambda| = 1$), that contain mutually orthonormal solutions (states) $\hat{X}_{\lambda,i}$ of the eigenvalue equation [7,9]

$$\widehat{U}_e^{(\phi)} \widehat{X}_{\lambda,i} \widehat{U}_e^{(\phi)\dagger} = \lambda \widehat{X}_{\lambda,i},\ \forall\, e \in M. \quad (10)$$

3. For known attractor spaces $\mathcal{A}_\lambda$ we get from an initial state $\hat{\rho}_{SE}^{in}$ the resulting S-E-state $\widehat{\rho}_{SE}^{out} = \widehat{\rho}_{SE}\,(N \gg 1)$ spanned by $\widehat{X}_{\lambda,i}$

$$\widehat{\rho}_{SE}^{out} = \mathcal{P}^N\left(\widehat{\rho}_{SE}^{in}\right) = \sum_{|\lambda|=1,\, i=1}^{d^\lambda} \lambda^N \mathrm{Tr}\left\{\widehat{\rho}_{SE}^{in} \widehat{X}_{\lambda,i}^\dagger\right\} \widehat{X}_{\lambda,i}, \quad (11)$$

where d^λ denotes the dimensionality of the attractor space $\mathcal{A}_\lambda$ w.r.t. the eigenvalue λ.

3.1 Minimal attractor space

What happens with Quantum Darwinism in the framework of the random unitary evolution model if we let the E-qubits interact with each other? From reference [7] we know that an ID with all mutually interacting E-qubits leads to the minimal attractor space structure (C.7) of Appendix C associated with an eigenvalue $\lambda = 1$ of (11). However, for this minimal $\lambda = 1$ attractor subspace of (11) to emerge one does not need to insist that *all* n E-qubits should interact with each other. It suffices to have a strongly connected ID that contains a closed arrow path between n E-qubits [7–9]. However, $2n-3$ is the critical (and maximal) number of $\widehat{u}_j^{(\phi)}$-bindings that one may insert between E-qubits into the ID of Figure 3 and still avoid the minimal $d^{\lambda=1}$ from (C.5) of Appendix C. Thus, for $\geq 2(n-1)$ $\widehat{u}_j^{(\phi)}$-bindings between E-qubits the corresponding ID remains strongly connected, leading always to the minimal $\lambda = 1$ attractor space (C.7) of Appendix C, whereas the $\lambda = -1$ attractor space of (11) vanishes already after inserting a single interaction arrow into environment E (see. Appendix C). Here we first turn to the physical interpretation of (C.7) from Appendix C.

3.1.1 State structure of the attractor space

The main differences between the maximal and the minimal $\lambda = 1$ attractor subspace (Eqs. (C.3) and (C.7) in Appendix C) that mainly determine the process of decoherence and transfer of $H(S_{class})$ to E are two-fold: (1) within the minimal $\lambda = 1$ attractor subspace (C.7) only the ground E-registry state $|0_n\rangle$ appears, whereas in (C.3) of the maximal $\lambda = 1$ attractor subspace all 2^n E-registry states contribute; (2) on the other hand, in (C.3) the E-registry states $|y\rangle$ are correlated within the diagonal S-subspace $|0_k\rangle\langle 0_k|$ only with each other, whereas (C.7) also allows the remaining E-registry state $|0_n\rangle$ to be correlated with the $\widehat{u}_j^{(\phi)}$-symmetry state $|s_{c_1}^n\rangle$. This means that effectively the contribution of the S-subspace $|0_k\rangle\langle 0_k|$ in equation (C.7) to $I(S:E_L)$, contrary to (C.3), becomes exponentially suppressed due to $|s_{c_1}^n\rangle$. The implications of this exponential, decoherence induced suppression of S-subspace $|0_k\rangle\langle 0_k|$ in equation (C.7) regarding quantum Darwinism will be discussed in the forthcoming subsection.

3.1.2 Results of the CNOT-evolution

Decomposing $\hat{\rho}_{SE}^{in}$ for $n \gg k$ S-qubits by means of (11) and (only) linear independent $\widehat{X}_{\lambda,i}$ from equation (C.7) of Appendix C, after first orthonormalizing all $\widehat{X}_{\lambda,i}$ in accord with the Gram-Schmidt algorithm, we obtain the CNOT-asymptotically evolved $\hat{\rho}_{SE}^{out}$ displayed in equations (D.6)–(D.10) of Appendix D.2. We consider in the following different inputs $\hat{\rho}_{SE}^{in}$ of the random unitary evolution and their PIPs obtained from the corresponding outputs $\hat{\rho}_{SE}^{out}$.

(I) $\hat{\rho}^{in}_{SE} = |\Psi^{in}_{S,\,k}\rangle\langle\Psi^{in}_{S,\,k}| \otimes \hat{\rho}^{in}_{E}$, $\hat{\rho}^{in}_{E} = |y\rangle\,\langle y|$, $y \in \{0_n,\, 1_n\}$

As usual, $\hat{\rho}^{in}_{S} = |\Psi^{in}_{S,\,k}\rangle\langle\Psi^{in}_{S,\,k}|$ is a pure k-qubit system. Numerous interesting conclusions can be obtained by looking at the behavior of MI with respect to the number n of E-qubits. For instance, within the maximal attractor space we need at least $n \geq 5$ E-qubits in order to see stable convergence of $I(S:E_{L=n})/H(S_{class})$, as indicated by the blue, •-dotted curve in Figure 4 associated with

$$\hat{\rho}^{in}_{SE} = \left|\Psi^{in}_{S,\,k=1}\right\rangle\left\langle\Psi^{in}_{S,\,k=1}\right| \otimes \hat{\rho}^{in}_{E},$$

where $|\Psi^{in}_{S,\,k=1}\rangle = \sum_{m=0}^{1} a_m|m\rangle$ ($|a_m|^2 = 2^{-1}\forall m$) is a pure $k=1$-qubit system S, $n > k = 1$ and $\hat{\rho}^{in}_{E} = |0_n\rangle\langle 0_n|$.

However, for the minimal $\lambda = 1$ attractor subspace the same input state $\hat{\rho}^{in}_{SE}$ leads for $k = 1$ to the output state in equation (D.6) of Appendix D.2 with non-zero eigenvalues

$$\begin{aligned}
\lambda^{SE}_{1} &= |a_1|^2\, 2^{-L} \quad \left(2^L - 1 \text{ times}\right)\\
\lambda^{SE}_{2/3} &= \left(2^{-1}\,|a_0|^2 + |a_1|^2\, 2^{-L+1}\right)\\
&\quad \pm \sqrt{2^{-2}\,|a_0|^4 + |a_1|^4\, 2^{-2(L+1)} - \epsilon_L}\\
\lambda^{E}_{1} &= |a_0|^2 + |a_1|^2\, 2^{-L}\\
\lambda^{E}_{2} &= |a_1|^2\, 2^{-L} \quad \left(2^L - 1 \text{ times}\right)\\
\lambda^{S}_{1/2} &= \frac{1}{2} \pm \sqrt{\frac{1}{4} - |a_0|^2\,|a_1|^2\,(1 - 2^{-2n})}
\end{aligned} \tag{12}$$

(valid $\forall\, 1 \leq L \leq n$), where

$$\epsilon_L := 2^{-2n+L}\left(2^{2(n-L)-1} - 1\right)|a_0|^2\,|a_1|^2\,.$$

The PIP of equation (12) is given by the yellow, ♦-dotted curve in Figure 6. Apparently, the absence of the $\lambda = -1$ attractor subspace is crucial for the appearance of Quantum Darwinism in case of $\hat{\rho}^{in}_{E} = |0_n\rangle\,\langle 0_n|$.

On the other hand, the ∘-dotted and the □-dotted curve in Figure 6 also demonstrate what happens within the minimal $\lambda = 1$ attractor subspace for the output state in equation (D.6) of Appendix D.2 with $k \geq 2$ S-qubits: since in the limit $n \gg k > 1$ (D.6) of Appendix D.2 leads to the same form (15) as (D.1) of Appendix D.1, we see that with increasing number k of S-qubits (i.e. in the limit $n \sim k \gg 1$) $I(S:E_{L=n})/H(S_{class})$ from equation (D.6) of Appendix D.2 will also behave (with $|a_i|^2 = 2^{-k}\,\forall i \in \{0,\ldots,2^k-1\}$) as

$$I\left(S:E_{L=n\sim k\gg 1}\right)/H\left(S_{class}\right) \sim 2^{-k}.$$

Accordingly, one also has (again with equal S-probability distribution $|a_i|^2 = 2^{-k}\,\forall i \in \{0,\ldots,2^k-1\}$)

$$I\left(S:E_{L=n\gg k\gg 1}\right)/H\left(S_{class}\right) = 0.$$

In Figure 4 we also see what happens with MI if $\hat{\rho}^{in}_{E}$, such as $\hat{\rho}^{in}_{E} = |1_n\rangle\langle 1_n|$, contains only E-registry states that do not participate within a given, in this case minimal $\lambda = 1$

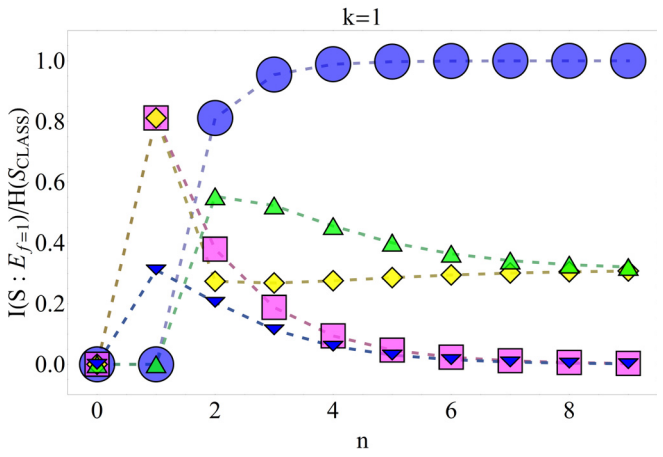

Fig. 4. $I(S:E_{L=n})/H(S_{class})$ vs n after random iterative $\widehat{u}_j^{(\phi=\pi/2)}$-evolution of $\hat{\rho}^{in}_{SE} = |\Psi^{in}_{S}\rangle\langle\Psi^{in}_{S}| \otimes \hat{\rho}^{in}_{E}$ ($N \gg 1$), with a $k=1$ qubit $|\Psi^{in}_{S}\rangle = \sum_{m=0}^{1} a_m|m\rangle$ ($|a_m|^2 = 2^{-1}\forall m$) and different $\hat{\rho}^{in}_{E}$ (with $\geq 2(n-1)$ E-bindings). $I(S:E_{L=n})/H(S_{class})$ vs. n for $\hat{\rho}^{in}_{E} = |0_n\rangle\langle 0_n|$ (blue, •-dotted curve, 0 E-bindings) is also displayed.

attractor subspace: $I(S:E_{L=n})/H(S_{class})$ (red, ■-dotted curve) tends to zero in the limit $n \gg k$. This can be easily explain by taking into account the fact that $\hat{\rho}^{out}_{SE_{L=n}}$ from equation (D.7) in Appendix D.2 acquires for a $k=1$ qubit S the form

$$\lim_{n\gg k}\hat{\rho}^{out}_{SE_{L=n}} = 2^{-n}\sum_{m=0}^{1}|a_m|^2\,|m\rangle\,\langle m| \otimes \widehat{I}_n, \tag{13}$$

in the limit $n \gg k$, yielding

$$H\left(S:E_{L=n\gg k}\right) = H\left(E_{L=n\gg k}\right) + H\left(S_{class}\right).$$

Thus, $\hat{\rho}^{in}_{E}$ that are not contained in ("recognized" by) a minimal $\lambda = 1$ attractor subspace do not contribute to $I(S:E_L)/H(S_{class})$ in the limit $n \gg k$.

(II) $\hat{\rho}^{in}_{SE} = |\Psi^{in}_{S,\,k=1}\rangle\langle\Psi^{in}_{S,\,k=1}| \otimes \frac{1}{2}\left(|0_n\rangle\,\langle 0_n| + |1_n\rangle\,\langle 1_n|\right)$

From Figure 4 (yellow, ♦-dotted curve) we also conclude that this type of $\hat{\rho}^{in}_{SE}$ never leads within the minimal $\lambda = 1$ attractor subspace to

$$I\left(S:E_{L=n}\right)/H\left(S_{class}\right) = 1$$

in the limit $n \gg k$, since in this case the corresponding $\hat{\rho}^{out}_{SE}$ from equation (D.8) in Appendix D.2 acquires the form

$$\begin{aligned}
\lim_{n\gg k}\hat{\rho}^{out}_{SE_{L=n}} = |a_0|^2\,|0\rangle\,\langle 0| \otimes \Big\{&\widehat{I}_n 2^{-n-1}\\
&+ \frac{1}{2}\,|0_n\rangle\,\langle 0_n|\Big\} + |a_1|^2\,|1\rangle\,\langle 1| \otimes 2^{-n}\cdot\widehat{I}_n,
\end{aligned} \tag{14}$$

which always yields

$$\lim_{n\gg k} H\left(S,\, E_{L=n}\right) > \lim_{n\gg k} H\left(E_{L=n}\right)$$

(as can be easily confirmed from the corresponding eigenspectra of $\lim_{n\gg k}\hat{\rho}^{out}_{SE_{L=n}}$ and $\lim_{n\gg k}\hat{\rho}^{out}_{SE}$, s. also Eq. (16) below). This means that correlation terms in equation (D.8) from Appendix D.2, that we deliberately ignored in equation (14), force the MI $I(S:E_{L=n})/H(S_{class})$ to converge to

$$I\left(S:\, E_{L=n}\right)/H\left(S_{class}\right) = 0.3$$

in the limit $n \gg k$. The same occurs if we choose

$$\left|\Psi^{in}_{E}\right\rangle = 2^{-1/2}\left(|0_n\rangle + |1_n\rangle\right)$$

as an environmental input state (green, ▲-dotted curve in Fig. 4), since its $\hat{\rho}^{out}_{SE}$ would acquire in the limit $n \gg k$ the same form equation (14). Thus, no Quantum Darwinism appears for these types of $\hat{\rho}^{in}_{E}$.

(III) $\hat{\rho}^{in}_{SE} = |\Psi^{in}_{S,\,k=1}\rangle\langle\Psi^{in}_{S,\,k=1}| \otimes 2^{-n}\hat{I}_n$

As in equation (17) below, $\hat{\rho}^{out}_{SE}$ from equation (D.9) of Appendix D.2 leads in the limit $n \gg k$ to

$$H\left(S,\, E_{L=n\gg k}\right) = H\left(S_{class}\right) + H\left(E_{L=n\gg k}\right),$$

i.e. completely mixed $\hat{\rho}^{in}_{E}$ leads also within the minimal $\lambda = 1$ attractor subspace to the MI-value

$$I\left(S:\, E_{L=n\gg k}\right)/H\left(S_{class}\right) = 0$$

(see Fig. 4, blue, ▼-dotted curve).

(IV) $\left|\Psi^{in}_{SE}\right\rangle = a\,|0_{k=1}\rangle \otimes \left|s_1^{L=n}\right\rangle + b\,|1_{k=1}\rangle \otimes \left|s_2^{L=n}\right\rangle$

The output state $\hat{\rho}^{out}_{SE}$ from equation (D.10) of Appendix D.2, emerging from the random unitary evolution of this entangled, pure input state $\hat{\rho}^{in}_{SE}$, and its eigenspectrum indicate that the relation

$$H\left(S,\, E_L\right) - H\left(E_L\right) = \frac{1}{2} + \left(1 - x_L\right)\log_2\left(1 - x_L\right) > 0,$$

where

$$x_L := 2^{n-L-1}\left(2^n - 1\right)^{-1},$$

holds for all $0 < L < n$. In other words, the corresponding PIP has the same behavior as displayed by the blue, ▼-dotted curve in Figure 5. Therefore, without the $\lambda = -1$ attractor subspace the minimal $\lambda = 1$ attractor subspace does not suffice to ensure that Quantum Darwinism appears, as is the case with the maximal attractor space discussed in Section 3.3 below.

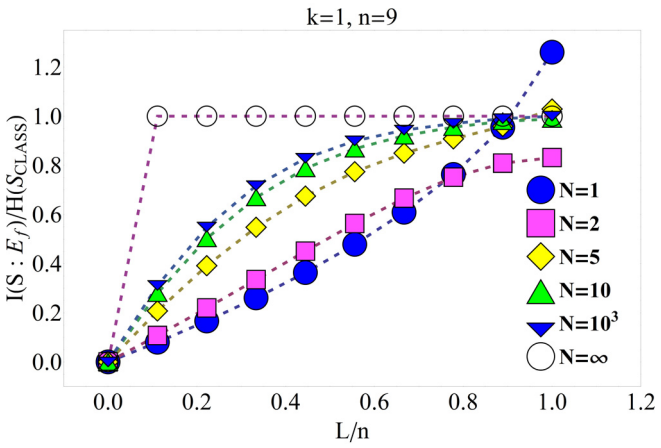

Fig. 5. PIP of simulated, random unitarily CNOT-evolved MI vs. $0 < f \leq 1$ for $\hat{\rho}^{in}_{SE} = \hat{\rho}^{in}_{S} \otimes \hat{\rho}^{in}_{E}$ in equation (4) and $\hat{\rho}^{out}_{SE}$ from equations (7)–(9). For $N = \infty$ see Section 3.3.2.

3.2 Short time limit of the random unitary evolution

Before looking at the analytic structure of the corresponding maximal attractor space we discuss whether one may interpret Zurek's qubit model of Quantum Darwinism as the short time limit (corresponding to the small number N of iterations) of the random unitary evolution involving pure decoherence.

Within the random unitary operation-formalism we obtain another type of PIP-behavior: inserting $\hat{\rho}^{in}_{SE}$ from Figure 1 into (9) we obtain for pure decoherence, with

$$|a|^2 = |b|^2 = 1/2$$
$$p_e = 1/|M|\ \forall e,$$

after $N \gg 1$ iterations the PIP in Figure 5, which suggests that Zurek's Quantum Darwinistic-"plateau" [3] appears only in the limit $N \to \infty$ (we will obtain this asymptotic limit $N \to \infty$ of the random unitary evolution analytically in Sect. 3.3). Thus, Zurek's qubit model of Quantum Darwinism does not appear as the short-time limit (small N-values, e.g. $N \leq 10$) of our random unitary evolution model with pure decoherence.

3.3 Maximal attractor space

When dealing with Koenig-IDs [11] we always obtain attractor (sub-)spaces with maximal dimension d^{λ} (determined by Eqs. (C.1)–(C.2) in Appendix C), since in such IDs E-qubits are not allowed to interact with each other. Therefore, we turn our attention in the following subsections to the description of analytical attractor space structures associated with Koenig-IDs and determined in Appendix C.

3.3.1 State structure of the attractor space

From Appendix C we know that for the random unitary evolution the attractor space consists of two subspaces (C.3) and (C.4) (Appendix C.1.2) associated with

eigenvalues $\lambda = 1$ and $\lambda = -1$ of equation (10), respectively.

The main (largest) part of the attractor states $\widehat{X}_{\lambda=1,i}$ can be attributed to the $|0_k\rangle\langle 0_k|$-subspace of system S, since the $\lambda = 1$-attractor subspace describes the impact of pure decoherence on system S during the iterative evolution (9) of $\hat{\rho}^{in}_{SE}$. However, in order to realize the physical significance of the $\lambda = -1$-attractor subspace we will discuss in the following subsection the random unitary evolution of some of the $\hat{\rho}^{in}_{SE}$ from Table A.1 that have already been studied in the course of Zurek's evolution in Section 2.

3.3.2 Results of the CNOT-evolution

Now we look at the random unitary CNOT-evolution from the analytical point of view by utilizing the attractor space structure from Section 3.3.1 and concentrating on the following input states $\hat{\rho}^{in}_{SE}$ (with $n \gg k \geq 1$):

$$\text{(I)}\ \hat{\rho}^{in}_{SE} = |\Psi^{in}_{S,k}\rangle\langle\Psi^{in}_{S,k}| \otimes \hat{\rho}^{in}_{E},\ \hat{\rho}^{in}_{E} = |y\rangle\langle y|,\ y \in \{0_n, 1_n\}$$

Decomposing $\hat{\rho}^{in}_{SE}$ for $n \gg k \in \{1, 2, 3\}$ S-qubits by means of equation (11) and $\widehat{X}_{\lambda,i}$ from equations (C.3)–(C.4) of Appendix C.1.2 that are already Gram-Schmidt orthonormalized, we obtain the CNOT-asymptotically evolved $\hat{\rho}^{out}_{SE}$ displayed in equation (D.1) of Appendix D.1. The corresponding PIP obtained from $\hat{\rho}^{out}_{SE}$ in equation (D.1) of Appendix D.1 for $k \in \{1, 2, 3\}$ S-qubits is displayed in Figure 6 below.

Figure 6 demonstrates that within the random unitary operations model Quantum Darwinism appears only for $k = 1$ pure $\hat{\rho}^{in}_{S}$ even if we set as an environmental input state $\hat{\rho}^{in}_{E} = |y\rangle\langle y|$ for all $y \in \{0, \ldots, 2^n - 1\}$ and with mutually non-interacting E-qubits, whereas for $n \sim k \gg 1$ the maximal $I(S : E_{L=n})$-value that can be achieved after enclosing the entire environment E behaves as

$$\lim_{n\sim k\gg 1} I\left(S : E_{L=n}\right)/H\left(S_{class}\right) \sim 2^{-k}.$$

This follows from equation (D.1) of Appendix D.1 which, with (without loss of generality) $|a_i|^2 = 2^{-k}\,\forall i \in \{0, \ldots, 2^k - 1\}$ and for $k > 1$, acquires in the limit $n \gg 1$ the form

$$\lim_{n\gg 1}\hat{\rho}^{out}_{SE_{L=n}} = |a_0|^2\,|0_k\rangle\langle 0_k| \otimes |0_n\rangle\langle 0_n| + \sum_{m=1}^{2^k-1} |a_m|^2\,|m\rangle\langle m| \otimes 2^{-n}\hat{I}_n. \qquad (15)$$

Equation (15) leads to $H(S) \approx H(S_{class}) = k$ (with a decoherence factor $0 \leq r = \langle s^n_1|\hat{\rho}^{in}_{E}|s^n_1\rangle = 2^{-n} \leq 1$), and non-zero eigenvalues

$$\lambda^{SE}_1 = |a_0|^2 = 2^{-k}\ \ (1\,\text{times})$$
$$\lambda^{SE}_2 = |a_m|^2\,2^{-n} = 2^{-(k+n)}\ \ \left(2^n\left[2^k - 1\right]\ \text{times}\right),$$

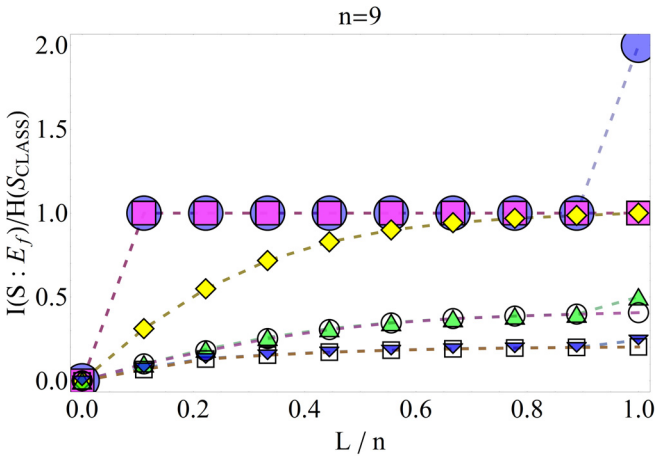

Fig. 6. PIP after random iterative $\widehat{u}^{(\phi=\pi/2)}_{j}$-evolution of $\hat{\rho}^{in}_{SE} = |\Psi^{in}_{S}\rangle\langle\Psi^{in}_{S}| \otimes |0_{n=9}\rangle\langle 0_{n=9}|$ $(N \gg 1)$, with a k qubit $|\Psi^{in}_{S}\rangle = \sum_{m=0}^{2^k-1} a_m|m\rangle$ $(|a_m|^2 = 2^{-k}\forall m)$, without $(k = 1,$ ■-dotted curve; $k = 2,$ ▲-dotted curve; $k = 3,$ ▼-dotted curve) and with ≥ 1 interaction bindings $(k = 1,$ ♦-dotted curve; $k = 2,$ ○-dotted curve; $k = 3,$ □-dotted curve) between E-qubits. The corresponding PIP of Zurek's model (•-dotted curve) is also displayed.

yielding (for fixed n and increasing k)

$$\lim_{n\sim k\gg 1} H\left(S, E_{L=n}\right) = 2k + k\cdot 2^{-k}.$$

Accordingly, the eigenvalues of $\lim_{n\gg 1}\hat{\rho}^{out}_{E_{L=n}}$ from equation (15),

$$\lambda^{E}_1 = |a_0|^2 + 2^{-n}\left(1 - |a_0|^2\right)\ \ (1\text{times})$$
$$\lambda^{E}_2 = 2^{-n}\left(1 - |a_0|^2\right)\ \ (\left[2^n - 1\right]\text{times}),$$

lead (as in Fig. 6) to

$$\lim_{n\sim k\gg 1} H\left(E_{L=n}\right) = k + k\cdot 2^{1-k}$$
$$\lim_{n\sim k\gg 1} I\left(S : E_{L=n}\right)/H\left(S_{class}\right) = 2^{-k}.$$

Even worse: if we choose k and n sufficiently high, such as $n \gg k \gg 1$, (15) yields (again with an S-probability distribution $|a_i|^2 = 2^{-k}\,\forall i \in \{0, \ldots, 2^k - 1\}$)

$$\lim_{n\gg k\gg 1} H\left(S, E_{L=n}\right) = k + n + k2^{-k}$$
$$\lim_{n\gg k\gg 1} H\left(E_{L=n}\right) = n + k2^{-k}$$
$$\lim_{n\gg k\gg 1} I\left(S : E_{L=n}\right)/H\left(S_{class}\right) = 0.$$

This is in conflict with the expectation of Zurek's CNOT-evolution model, which predicts the appearence of the MI-'plateau' $\forall k \geq 1$. Apparently, the random unitary evolution model suggests that in order to store $H(S_{class})$ into environment E efficiently one needs environments consisting of qudit-cells (2^k-level systems). This conjecture

is also supported by equation (B.6) in Appendix B, which indicates that for Quantum Darwinism to appear w.r.t. $k > 1$ one needs 2^k symmetry states. Unfortunately, the qubit-qubit $\widehat{u}_j^{(\phi)}$-transformation in equations (7)–(8) (and thus also the CNOT) offers only two symmetry states $\{|s_{c_1}\rangle, |s_{c_2}\rangle\}$. Therefore, one would require a qubit-qudit version of equations (7)–(8) in order to see Quantum Darwinism.

On the other hand, for $k = 1$ $\hat{\rho}_{SE_L}^{out}$ and $\hat{\rho}_{E_L}^{out}$ from equation (D.1) in Appendix D.1 have $\forall(1 \leq L \leq n)$ identical non-zero eigenvalues

$$\begin{aligned}\lambda_1^{(S)E} &= |a_1|^2 2^{-L} \ (\left[2^L - 1\right] \text{ times})\\ \lambda_2^{(S)E} &= 2^{-1}|a_0|^2 + 2^{-(L+1)}|a_1|^2\\ &\quad + \sqrt{\left(2^{-1}|a_0|^2 + |a_1|^2 2^{-(L+1)}\right)^2 - g_N}\\ &= |a_0|^2 + 2^{-L}|a_1|^2 \ (1 \text{ times}),\end{aligned}$$

with

$$g_N := |a_0|^2 |a_1|^2 2^{-2n+L} \left[\underbrace{1 - (-1)^{2N}}_{:=0}\right],$$

due to the $\lambda = -1$ attractor subspace and its contributions in $\lambda_2^{(S)E}$ proportional to $(-1)^{2N}$ and characterized by the iteration number N from equation (11). Again, $H(S) \approx H(S_{class})$ for $n \gg k$ due to eigenvalues

$$\lambda_{1/2}^S = 1/2 \pm \sqrt{1/4 - \left(1 - 2^{-2n}\left[1 + (-1)^N\right]^2\right)|a_0|^2|a_1|^2}$$

of $\hat{\rho}_S^{out}$ from equation (D.1) in Appendix D.1.

(II) $\hat{\rho}_{SE}^{in} = |\Psi_{S,\,k=1}^{in}\rangle\langle\Psi_{S,\,k=1}^{in}| \otimes \frac{1}{2}\left(|0_n\rangle\langle 0_n| + |1_n\rangle\langle 1_n|\right)$

The PIP obtained from a random unitarily $\widehat{u}_j^{(\phi=\pi/2)}$-evolved $\hat{\rho}_{SE}^{out}$ in equation (D.2) of Appendix D.1 for $k = 1$ S-qubit is displayed in Figure 7 below (red, ■-dotted curve). We see that if $\hat{\rho}_E^{in}$ contains correlations between E-registry states one is even not able to extract $H(S_{class})$ after taking the entire E into account when computing $I(S:E_L)$, since according to Figure 7

$$I(S:E_{L=n})/H(S_{class}) < 1.$$

This can be easily explained by looking at the $n \gg k$ limit of equation (D.2) in Appendix D.1

$$\begin{aligned}\lim_{n\gg k}\hat{\rho}_{SE_{L=n}}^{out} &= |a_0|^2|0_k\rangle\langle 0_k| \otimes \hat{\rho}_E^{in}\\ &\quad + |a_1|^2|1\rangle\langle 1| \otimes 2^{-n}\hat{I}_n\\ &\Rightarrow H(S) = H(S_{class})\\ \lim_{n\gg k}\hat{\rho}_{E_{L=n}}^{out} &= |a_0|^2\hat{\rho}_E^{in} + |a_1|^2 2^{-n}\hat{I}_n. \qquad (16)\end{aligned}$$

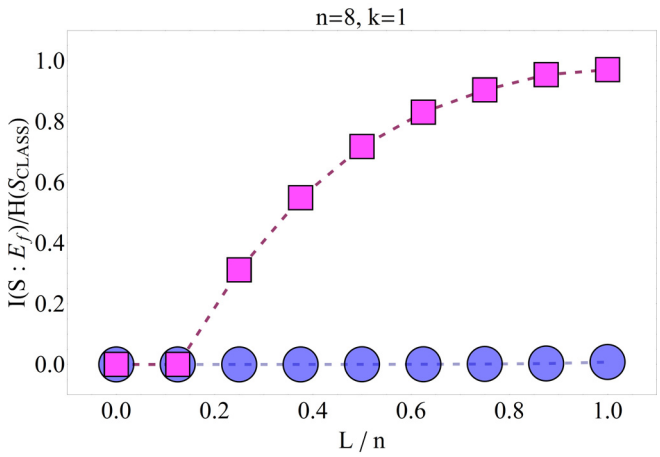

Fig. 7. PIP after random iterative $\widehat{u}_j^{(\phi=\pi/2)}$-evolution of $\hat{\rho}_{SE}^{in} = |\Psi_S^{in}\rangle\langle\Psi_S^{in}| \otimes \hat{\rho}_E^{in}$ $(N \gg 1)$, with a pure $k = 1$ qubit $|\Psi_S^{in}\rangle = \sum_{m=0}^{1} a_m|m\rangle$ $(|a_m|^2 = 2^{-1}\forall m)$, $n = 8$ and different $\hat{\rho}_E^{in}$ (0 E-bindings), see main text.

The (non-zero) eigenvalues

$$\begin{aligned}\lambda_1^{SE} &= |a_0|^2 2^{-1} \ (2 \text{ times})\\ \lambda_2^{SE} &= |a_1|^2 2^{-n} \ (2^n \text{ times})\end{aligned}$$

(for $\lim_{n\gg k}\hat{\rho}_{SE_{L=n}}^{out}$), as well as eigenvalues

$$\begin{aligned}\lambda_1^E &= |a_0|^2 2^{-1} + |a_1|^2 2^{-n} \ (2 \text{ times})\\ \lambda_2^E &= |a_1|^2 2^{-n} \ (\left[2^n - 2\right] \text{ times})\end{aligned}$$

(for $\lim_{n\gg k}\hat{\rho}_{E_{L=n}}^{out}$), yield (for $0 < |a_0|^2 < 1$)

$$\begin{aligned}\lim_{n\gg k} H(S, E_{L=n}) &= H(S_{class}) + |a_0|^2\\ &\quad + |a_1|^2 n > \lim_{n\gg k} H(E_{L=n}),\end{aligned}$$

since $\lim_{n\gg k} H(E_{L=n})$ contains two addends,

$$\begin{aligned}A_1 :&= -|a_1|^2 \log_2 \frac{|a_1|^2}{2^n} + 2^{1-n}|a_1|^2 \log_2 \frac{|a_1|^2}{2^n}\\ A_2 :&= -\left(|a_0|^2 + 2^{1-n}|a_1|^2\right)\\ &\quad \times \log_2\left(2^{-1}|a_0|^2 + 2^{-n}|a_1|^2\right),\end{aligned}$$

with

$$\begin{aligned}A_1 &< -|a_1|^2 \log_2 \frac{|a_1|^2}{2^n}\\ A_2 &< -|a_0|^2 \log_2 \frac{|a_0|^2}{2}.\end{aligned}$$

In other words, if correlations between E-registry states persist throughout the process of tracing out E-qubits from $\hat{\rho}_{SE_{L=n}}^{out}$, equation (5) will be violated and the MI-'plateau' disappears, confirming the corresponding results

obtained by means of Zurek's model of Quantum Darwinism (see also discussion from Sect. 3.4 below). Effectively the same PIP emerges if one starts the above random unitary evolution with

$$\left|\Psi_E^{in}\right\rangle = 2^{-1/2}\left(|0_n\rangle + |1_n\rangle\right),$$

since contributions within the corresponding $\hat{\rho}_{SE}^{out}$ associated with non-classical correlation terms $|0_n\rangle\langle 1_n|$ and $|1_n\rangle\langle 0_n|$ also vanish in the limit $n \gg k$ for all $(k \leq L < n)$.

(III) $\hat{\rho}_{SE}^{in} = |\Psi_{S,\,k=1}^{in}\rangle\langle\Psi_{S,\,k=1}^{in}| \otimes 2^{-n}\hat{I}_n$

An extreme case for $\hat{\rho}_E^{in}$ containing classical correlations between E-registry states is the totally mixed environmental n-qubit input state which leads according to Figure 7 (blue, •-dotted curve) to

$$\lim_{n\gg k} I\left(S:\, E_{L=n}\right)/H\left(S_{class}\right) \approx 0.$$

This follows from the $n \gg k$ limit

$$\lim_{n\gg k}\hat{\rho}_{SE_{L=n}}^{out} = \left(|a_0|^2\,|0_k\rangle\,\langle 0_k| + |a_1|^2\,|1\rangle\,\langle 1|\right)\otimes 2^{-n}\hat{I}_n$$
$$\Rightarrow H\left(S,\, E_{L=n\gg k}\right) = H\left(S_{class}\right) + H\left(E_{L=n\gg k}\right) \qquad (17)$$

of equation (D.3) in Appendix D.1. In other words, completely mixed $\hat{\rho}_E^{in}$ are not suitable for efficiently storing $H(S_{class})$ into E with $f \leq k/n$.

(IV) $\hat{\rho}_{SE}^{in} = |\Psi_{S,\,k=1}^{in}\rangle\langle\Psi_{S,\,k=1}^{in}| \otimes \frac{(|0_n\rangle\langle 0_n| + |10_{n-1}\rangle\langle 10_{n-1}|)}{2}$

This type of $\hat{\rho}_E^{in}$ leads within the random unitary model to $\hat{\rho}_{SE}^{out}$ in equation (D.4) of Appendix D.1, demonstrating that within the random unitary model it is, as was the case with Zurek's model, in principle important in which order one traces out single E-qubits: if we trace out the first left E-qubit in $|10_{n-1}\rangle\langle 10_{n-1}|$ for a fixed L-value $L = L^*$ with $k \leq L^* < n$, $\hat{\rho}_{SE_{L^*}}^{out}$ in equation (D.4) of Appendix D.1 would reduce to $\hat{\rho}_{SE_{L^*}}^{out}$ from equation (D.1) of Appendix D.1, validating (5) at least $\forall(k \leq L \leq L^*)$.

However, in general this is not what we demand from $\hat{\rho}_{SE}^{out}$ whose E should allow complete reconstruction of the "classical" entropy $H(S_{class})$ regardless of the order in which one decides to intercept environmental fragments (qubits). This implies that among all possible combinations (sums) of E-registry states only the pure (one) E-registry state $\hat{\rho}_E^{in} = |y\rangle\langle y|$ in the standard computational basis (for all $y \in \{0, \ldots 2^n - 1\}$) leads to quantum Darwinism, both in Zurek's and the random unitary model.

(V) $\left|\Psi_{SE}^{in}\right\rangle = a\,|0_{k=1}\rangle \otimes \left|s_1^{L=n}\right\rangle + b\,|1_{k=1}\rangle \otimes \left|s_2^{L=n}\right\rangle$

This artificial $\hat{\rho}_{SE}^{in}$ entangles each S-pointer state with one of the $\widehat{u}_j^{(\phi)}$-symmetry states $\{|s_{c_1}^L\rangle, |s_{c_2}^L\rangle\}$, validating (5), according to Appendix B, only for $c_1 = c_2 = 1/2$, which is why we obtain for the corresponding $\hat{\rho}_{SE}^{out}$ in equation (D.5) of Appendix D.1 exactly the same PIP as the one displayed in Figure 1: $\hat{\rho}_{SE}^{in}$ simply does not change $\forall N \gg 1$ due to invariance of E towards $\widehat{u}_j^{(\phi=\pi/2)}$ and the fact that the $\lambda = -1$ attractor subspace in equation (C.4) of Appendix C.1.2 contributes to the random unitary evolution of $\hat{\rho}_{SE}^{in}$ for a $k = 1$ qubit system S only a phase $(-1)^N$-factor within the $|0\rangle\langle 1|$- and $|1\rangle\langle 0|$-subspace of system S.

For $k > 1$ one could obtain Quantum Darwinism according to equations (C.3)–(C.4) (Appendix C.1.2) only if one entangles two S-pointer states $\{|0_{k>1}\rangle, |1_{k>1}\rangle\}$ with available CNOT-symmetry states $\{|s_1^L\rangle, |s_2^L\rangle\}$. However, this would enable us to store only

$$0 < H\left(S\right) = H\left(S_{class}\right) \leq 1,$$

corresponding to a $k = 1$ qubit system S. In order to store $H(S_{class})$ of a $k > 1$ qubit S one needs 2^k symmetry states of $\widehat{U}_{ij}^{(\phi)}$ (Eq. (7) above) with which one could entangle the 2^k S-pointer states $\{|\pi_i\rangle\} \equiv \{|i\rangle\}_{i=0}^{i=2^k-1}$, otherwise if the number of S-pointer states exceeds the number of available $\widehat{U}_{ij}^{(\phi)}$-symmetry states, Quantum Darwinism disappears (Eqs. (B.4)–(B.6) in Appendix B).

3.4 MI-Comparison: maximal vs. minimal attractor space

Here we inquire which conclusions about the MI-behavior regarding an increasing number of environmental qubit-qubit $\widehat{u}_j^{(\phi=\pi/2)}$-interactions can be drawn simply by comparing the PIPs associated with both extrema – the minimal and maximal attractor subspaces associated with an eigenvalue $\lambda = 1$ of equation (11).

Indeed, many important conclusions about the behavior of the MI with increasing number of E-qubit interactions in Figure 3 can be drawn from a simple comparison between predictions obtained by the random unitary evolution of $\hat{\rho}_{SE}^{in}$ in Figure 1 from the point of view of the minimal and the maximal $\lambda = 1$ attractor subspaces (C.3) and (C.7) (Appendices C.1.2 and C.2.2), respectively. For instance, looking at the PIP associated with the maximal $\lambda = 1$ attractor subspace (C.3) alone (for a $k \geq 1$ qubit system S (s. Appendix C.1.2)), which we obtain by ignoring all addends in $\hat{\rho}_{SE}^{out}$ of equation (D.1) from Appendix D.1 proportional to $(-1)^N$, we see that the MI behaves as in the PIP emerging from $\hat{\rho}_{SE}^{out}$ in equation (D.6) of Appendix D.2 evolved with respect to the minimal $\lambda = 1$ attractor subspace. In other words, the PIP for $\hat{\rho}_{SE}^{out}$ (and a $k \geq 1$ qubit system S) in equation (D.1) of Appendix D.1 without contributions associated with the $\lambda = -1$ attractor subspace and the PIP obtained from $\hat{\rho}_{SE}^{out}$ in equation (D.6) (Appendix D.2) of the minimal $\lambda = 1$ attractor subspace are exactly the same and are given by the ♦-, ○- and □-dotted curves in Figure 6 (this can also be confirmed numerically by iterating (9) $N \gg 1$ times).

This means: $\hat{\rho}_{SE}^{out}$ from the $\lambda = 1$-part of equation (D.1) in Appendix D.1 and $\hat{\rho}_{SE}^{out}$ in equation (D.6) of Appendix D.2, as can be readily confirmed, share the same

non-zero eigenvalues (12). The presence of the $\lambda = -1$ attractor subspace (C.4) from Appendix C.1.2 in equation (D.1) of Appendix D.1 is essential for the appearence of Quantum Darwinism (for a $k = 1$ qubit system S) within the random unitary model. Since the $\lambda = -1$ attractor subspace disappears from the attractor space structure of a Koenig-like ID already after introducing a single interaction arrow between two E-qubits (s. Appendix C), the PIP of a random unitarily evolved $\hat{\rho}_{SE}^{in}$ from Figure 1 for environments E containing one or more $\widehat{u}_j^{(\phi=\pi/2)}$-bindings should be the same as the PIP of obtained from equation (D.6) of Appendix D.2 for the minimal $\lambda = 1$ attractor space, i.e. already a single interaction between E-qubits in ID of Figure 3 destroys Quantum Darwinism in the random unitary model.

For $\hat{\rho}_E^{in} \neq |y\rangle\langle y| \; \forall y \in \{0, \ldots, 2^n - 1\}$ the contribution of the $\lambda = -1$ attractor subspace (C.4) within the maximal attractor space (C.3)–(C.4) from Appendix C.1.2 to the random unitary evolution of $\hat{\rho}_{SE}^{in} = \hat{\rho}_S^{in} \otimes \hat{\rho}_E^{in}$ and its MI-values is negligibly small in the limit $L = n \gg k$, whereas the attractor subspace (C.3) of Appendix C.1.2 and its minimal version (C.7) from Appendix C.2.2 dominate the asymptotic dynamics of $\hat{\rho}_{SE}^{in}$.

Nevertheless, contributions from the $\lambda = -1$ attractor subspace do affect outer-diagonal S-subspaces. For instance, equation (D.2) in Appendix D.1 contains the most important part of the $\lambda = -1$ attractor subspace, namely

$$\left\{|0_L\rangle\left\langle s_2^L\right|, |1_L\rangle\left\langle s_2^L\right|\right\}$$

(and their hermitean counterparts), within S-subspaces $|0\rangle\langle 1|$ and $|1\rangle\langle 0|$. When looking at equation (D.2) in Appendix D.1 we see that these outer-diagonal S-subspaces are associated with matrix entries

$$\left[|0_L\rangle + |1_L\rangle\right]\left\langle \Psi_E^{combi}\right|$$

(and their hermitean counterpart, respectively), where

$$\left|\Psi_E^{combi}\right\rangle = \left|s_1^L\right\rangle + (-1)^{2n-L+N}\left|s_2^L\right\rangle$$

distributes within the $|0_L\rangle$th and $|1_L\rangle$th row (column) of equation (D.2) in Appendix D.1 2^{L-1} complex-valued, identical entries $c = 2^{1-n}a_0a_1^*$ (alias its conjugate counterparts). If we ask ourselves what is the ideal value c_{ideal} of these 2^{L-1} identical entries in equation (D.2) of Appendix D.1, distributed within the $|0_L\rangle$th and $|1_L\rangle$th row (column) in accord with $\left|\Psi_E^{combi}\right\rangle$, for which the entropy-difference with respect to $\hat{\rho}_{SE}^{out}$ and $\hat{\rho}_E^{out}$, $H\left(S, E_{L=n}\right) - H\left(E_{L=n}\right)$ (with $n \gg k$), is minimal, we easily obtain

$$c_{ideal} = 2^{-n}a_0a_1^* \neq 2^{1-n}a_0a_1^*,$$

leading us for $\hat{\rho}_{SE}^{out}$ in equation (D.2) of Appendix D.1 to eigenvalues

$$\left.\begin{array}{c}\lambda_1^{SE} = 2^{-1}\left|a_0\right|^2 \\ \lambda_2^{SE} = 2^{1-L}\left|a_1\right|^2\left(2^{L-1} - 1 \text{ times}\right)\end{array}\right\} (\text{for } \hat{\rho}_{SE}^{out})$$

$$\left.\begin{array}{c}\lambda_1^{E} = 2^{-1}\left|a_0\right|^2 + 2^{1-L}\left|a_1\right|^2 \; (2 \text{ times}) \\ \lambda_2^{E} = 2^{1-L}\left|a_1\right|^2\left(2^{L-1} - 2 \text{ times}\right)\end{array}\right\} (\text{for } \hat{\rho}_E^{out}), \quad (18)$$

that, in turn, yield $H(S, E_{L=n}) > H(E_{L=n})$. In other words, even in case of outer-diagonal c-entries in equation (D.2) from Appendix D.1 fixed as $c = c_{ideal}$ $H(S, E_{L=n})$ would still always exceed $H(E_{L=n})$.

The reason for this is connected with the following fact: for equation (D.1) of Appendix D.1, emerging from the random unitary CNOT-evolution of $\hat{\rho}_E^{in} = |0_n\rangle\langle 0_n|$, the diagonal value $|a_0|^2$ from the diagonal S-subspace $|0\rangle\langle 0|$ in equation (D.1) of Appendix D.1 merges with one of the diagonal values $2^{-L}|a_1|^2$ from the diagonal S-subspace $|1\rangle\langle 1|$ after extracting $\hat{\rho}_E^{out}$ from $\hat{\rho}_{SE}^{out}$ and thus decreases $H(E_L)$ with respect to $H(S, E_L)$. Fortunately, for this case $|\Psi_E^{combi}\rangle$ is the only combination that ca be made from two available CNOT-symmetry states $\{|s_1^L\rangle, |s_2^L\rangle\}$ capable of reducing $H(S, E_L)$ such that $H(S, E_L) = H(E_L) \forall (1 \leq L \leq n)$. Unfortunately, in order to correct a higher number of overlapping diagonal values between S-subspaces $|0\rangle\langle 0|$ and $|1\rangle\langle 1|$ within $\hat{\rho}_E^{out}$ (in Eq. (D.2) of Appendix D.1 there are two merging diagonal values between S-subspaces $|0\rangle\langle 0|$ and $|1\rangle\langle 1|$) one would also need more than two symmetry states which is impossible for the CNOT transformation and, in general, for the ϕ-parameter family $\widehat{u}_j^{(\phi)}$ of transformations in equations (7)–(8) (however, a higher number of symmetry states is possible for a generalized, qudit-qudit version of the CNOT-transformation).

Therefore, $\hat{\rho}_{SE}^{in} = \hat{\rho}_S^{in} \otimes \hat{\rho}_E^{in}$ (with $\hat{\rho}_S^{in}$ being a pure $k = 1$ qubit system S), when being subject to CNOT-random unitary evolution leads in the asymptotic limit $N \gg 1$ of many iterations to Quantum Darwinism only if $\hat{\rho}_E^{in} = |y\rangle\langle y| \forall y \in \{0, \ldots, 2^n - 1\}$, otherwise, for E-input states $\hat{\rho}_E^{in} \neq |y\rangle\langle y| \forall y \in \{0, \ldots, 2^n - 1\}$ the $\lambda = -1$ attractor subspace (C.4) of Appendix C.1.2 does not suffice to compensate all losses of $H(E_L)$ induced in $\hat{\rho}_E^{out}$ by overlapping diagonal entries within different diagonal S-subspaces.

Furthermore, by comparing the ■-dotted curve in Figure 7 with the ♦-dotted curve in Figure 4 we may conclude that the highest amount of asymptotic MI-values one could achieve $\forall (k \leq L \leq n)$ is bounded from above by $I(S : E_L)$ obtained from the maximal attractor space (C.3)–(C.4) of Appendix C.1.2.

4 Summary and outlook

In this paper we studied the appearence of quantum Darwinism in the framework of the random unitary qubit model and compared the corresponding results (Partial Information Plots of mutual information between an open $k \geq 1$ qubit system S and its $n \gg k$ qubit environment E) with respective predictions obtainable from Zurek's qubit toy model.

We found that the only S-E-input states $\hat{\rho}_{SE}^{in}$ which lead to Quantum Darwinism within the random unitary operations model with maximal efficiency $f = f^* = k/n$, regardless of the order in which one traces out single E-qubits, are the entangled input state from equation (6) and the product state $\hat{\rho}_{SE}^{in} = \hat{\rho}_S^{in} \otimes \hat{\rho}_E^{in}$, with a pure $k = 1$

qubit $\hat{\rho}_S^{in}$ and a pure one-registry state $\hat{\rho}_E^{in} = |y\rangle\langle y| \; \forall y \in \{0, \ldots, 2^n - 1\}$ of n mutually non-interacting qubits in the standard computational basis (Koenig-IDs).

According to the random unitary operations model one is motivated to conjecture that $\hat{\rho}_{SE}^{in} = \hat{\rho}_S^{in} \otimes \hat{\rho}_E^{in}$ with a pure $k > 1$ qubit $\hat{\rho}_S^{in}$ allows efficient storage of system's Shannon-entropy $H(S_{class})$ into environment E only if $\hat{\rho}_E^{in}$ is given by a pure one registry state $\hat{\rho}_E^{in} = |y'\rangle\langle y'|$ of mutually non-interacting n qudits (n 2^k-level systems) in the standard computational basis, with $y' \in \{0, \ldots, 2^{k \cdot n} - 1\}$.

This does not correspond to expectations arising from Zurek's qubit model of Quantum Darwinism, which predicts the appearence of the mutual information-'plateau' even for a $k > 1$ qubit pure $\hat{\rho}_S^{in}$ and an n qubit $\hat{\rho}_E^{in}$ within the aforementioned $\hat{\rho}_{SE}^{in} = \hat{\rho}_S^{in} \otimes \hat{\rho}_E^{in}$, indicating that Quantum Darwinism depends on the specific model on which one bases his interpretations. Furthermore, the random unitary model and Zurek's model of Quantum Darwinism must not be confused with each other, since the latter does not correspond to the short time limit (small iteration values N) of the former.

On the other hand, both in Zurek's and the random unitary model we are able to confirm that correlations between qubit E-registry states in $\hat{\rho}_E^{in}$, even if interactions between E-qubits are absent, tend to suppress the appearence of the mutual information-'plateau'. Also, the random unitary model indicates that already a single interaction between E-qubits suppresses quantum Darwinism.

If the Quantum Darwinistic description of the emergence of classical S-states were correct, then Zurek's and the random unitary model suggest that an open (observed) system S of interest and its environment E must have started their evolution as a product state $\hat{\rho}_{SE}^{in} = \hat{\rho}_S^{in} \otimes \hat{\rho}_E^{in}$ with $\hat{\rho}_S^{in}$ denoting a pure $k \geq 1$ qubit state and $\hat{\rho}_E^{in}$ (denoting for instance the state of the rest of the universe) given by a pure one-registry state of mutually non-interacting n qudits.

The above "qudit-cell" conjecture regarding environment E of the random unitary model could be tested by explicitly determining the maximal attractor space between a $k > 1$ qubit system S and its environment E of mutually non-interacting n qudits under the impact of the generalized qubit-qudit version of the CNOT transformation and focussing on the behavior of the mutual information within the corresponding Partial Information Plot for such maximal attractor space (Koenig-IDs). Furthermore, one could also ask what happens with the efficiency of storing $H(S_{class})$ into environment E if one introduces into the above random unitary evolution with pure decoherence dissipative effects that would in general treat the system S in the interaction digraph of Figure 3 not only as a control but also as a target, allowing E-qubits to react on "impulses" sent by S-qubits (paper in preparation).

Author contribution statement

The results of this paper were obtained by the author (N. Balanesković) in the framework of his Ph.D.-research.

The author thanks G. Alber, J. Novotný and J. Rennes for stimulating discussions.

Appendix A: List of exemplary input and output states in Zurek's model of Quantum Darwinism

In the present appendix we list all exemplary environmental input states in $\hat{\rho}_{SE}^{in} = \hat{\rho}_S^{in} \otimes \hat{\rho}_E^{in}$ and their output states $\hat{\rho}_{SE_L}^{out}$ discussed in the course of Zurek's qubit model of Quantum Darwinism in Section 2, Figure 2.

Appendix B: Quantum Darwinism and eigenstates of (7)–(8)

In this appendix we explain why the generalized $k > 1$ qubit version of equation (6) does not lead to Quantum Darwinism.

The ϕ-parameter family $\widehat{u}_j^{(\phi)}$ of transformations in equations (7)–(8) has eigenstates $|s_{c_1}\rangle = (c_1|0\rangle + c_2|1\rangle)$ (eigenvalue $\lambda = 1$) and $|s_{c_2}\rangle = (c_2|0\rangle - c_1|1\rangle)$ (eigenvalue $\lambda = -1$), with $\langle s_{c_1}|s_{c_2}\rangle = 0$ and $c_1^2 + c_2^2 \stackrel{!}{=} 1$ ($c_1, c_2 > 0$) [7–9]. This allows us to parametrize

$$c_1 = \cos\left(\frac{\phi}{2}\right), \; c_2 = \sin\left(\frac{\phi}{2}\right)$$

and thus fix ϕ within the range ($0 \leq \phi \leq \pi$). By means of this ϕ-parametrization we may generalize (6) according to

$$\begin{aligned} \left|\Psi_{SE}^{out}(L=n)\right\rangle &= a\,|0\rangle \otimes \left|s_{c_1}^L\right\rangle + b\,|1\rangle \otimes \left|s_{c_2}^L\right\rangle \\ \hat{\rho}_E^{out}(L=n) &= |a|^2 \left|s_{c_1}^L\right\rangle\left\langle s_{c_1}^L\right| + |b|^2 \left|s_{c_2}^L\right\rangle\left\langle s_{c_2}^L\right|, \end{aligned} \quad \text{(B.1)}$$

with

$$\left|s_{c_1}^L\right\rangle = |s_{c_1}\rangle^{\otimes L}, \; \left|s_{c_2}^L\right\rangle = |s_{c_2}\rangle^{\otimes L}, \; \left\langle s_{c_1}^L|s_{c_2}^L\right\rangle = 0.$$

For $L = n$ one would always obtain $H(S) = H(S_{class})$ and $H(S, E_{L=n}) = 0 < H(E_{L=n})$, since (B.1) is a pure state, whereas the spectrum of $\hat{\rho}_E^{out}(L = n)$ would, for simplicity for $L = n = 1$, contain the non-vanishing eigenvalues

$$\lambda_{1/2}^{E(L=n=1)} = \frac{1}{2} \pm \sqrt{\frac{1}{4} - 4c_1^2 c_2^2 |a|^2 |b|^2}.$$

Tracing out E-qubits in equation (B.1) forces $\hat{\rho}_{SE_L}^{out}$ to acquire the form

$$\begin{aligned} \hat{\rho}_{SE}^{out}(L<n) = |a|^2 |0\rangle\langle 0| \otimes \left|s_{c_1}^L\right\rangle\left\langle s_{c_1}^L\right| \\ + |b|^2 |1\rangle\langle 1| \otimes \left|s_{c_2}^L\right\rangle\left\langle s_{c_2}^L\right|, \end{aligned} \quad \text{(B.2)}$$

Table A.1. $\hat{\rho}^{out}_{SE_L}$ from Zurek's CNOT-evolution of $\hat{\rho}^{in}_{SE} = \hat{\rho}^{in}_{S} \otimes \hat{\rho}^{in}_{E}$ for different $\hat{\rho}^{in}_{E}$ (s. Fig. 2).

$\hat{\rho}^{in}_{E}$	$\hat{\rho}^{out}_{SE_L}$/entropies
(1) $\frac{1}{2}(\|0_n\rangle\langle 0_n\| + \|0_{n-1}1\rangle\langle 0_{n-1}1\|)$ $H(S) = H(S_{class})\ \forall L$ • – dotted curve	$\|a\|^2 \|0\rangle\langle 0\| \otimes \hat{\rho}^{in}_{E}$ $+\frac{1}{2}\|b\|^2 \|1\rangle\langle 1\| \otimes (\|1_n\rangle\langle 1_n\| + \|1_{n-1}0\rangle\langle 1_{n-1}0\|)$ $+\frac{1}{2}ab^* \|0\rangle\langle 1\| \otimes (\|0_n\rangle\langle 1_n\| + \|0_{n-1}1\rangle\langle 1_{n-1}0\|)$ $+\frac{1}{2}a^*b \|1\rangle\langle 0\| \otimes (\|1_n\rangle\langle 0_n\| + \|1_{n-1}0\rangle\langle 0_{n-1}1\|)$ $\begin{cases} H_{SE} = H(S_{class}) + \delta_{L,n} \\ H_E = (1-\delta_{L,n}) H(S_{class}) \\ +\delta_{L,n}\ (1 \le L \le n) \end{cases}$
(2) $\frac{1}{2}(\|0_n\rangle\langle 0_n\| + \|10_{n-1}\rangle\langle 10_{n-1}\|)$ $H(S) = H(S_{class})\ \forall L$ ■ – dotted curve	as in 1), with $\|0_{n-1}1\rangle \leftrightarrow \|10_{n-1}\rangle$ $\|1_{n-1}0\rangle \leftrightarrow \|01_{n-1}\rangle$ $\begin{cases} H_{SE} = (1-\delta_{L,n}) H(S_{class}) + 1\ (1 \le L \le n) \\ H_E = 1 \text{ for } L = 1 \\ H_E = (1-\delta_{L,n}) H(S_{class}) + H_{SE}\ (2 \le L \le n) \end{cases}$
(3) $\frac{1}{2}(\|0_n\rangle\langle 0_n\| + \|1_n\rangle\langle 1_n\|)$ $H(S) = H(S_{class})\ \forall L$ ♦ – dotted curve	$(\|a\|^2 \|0\rangle\langle 0\| + \|b\|^2 \|1\rangle\langle 1\|) \otimes \hat{\rho}^{in}_{E}$ $+\frac{1}{2}(ab^* \|0\rangle\langle 1\| + a^*b \|1\rangle\langle 0\|)$ $\otimes (\|0_n\rangle\langle 1_n\| + \|1_n\rangle\langle 0_n\|)$ $\begin{cases} (1 \le L \le n):\ H_E = 1 \\ H_{SE} = (1-\delta_{L,n}) H(S_{class}) + 1 \end{cases}$
(4) $2^{-n}\hat{I}_n = \left(2^{-1}\hat{I}_1\right)^{\otimes n}$ $\{\|x\rangle, \|y\rangle\} \in \{0, \ldots, 2^n - 1\}$ $H(S) = H(S_{class})\ \forall L$ ♦ – dotted curve	$(\|a\|^2 \|0\rangle\langle 0\| + \|b\|^2 \|1\rangle\langle 1\|) \otimes \hat{\rho}^{in}_{E}$ $+2^{-n}ab^* \|0\rangle\langle 1\| \otimes \sum_{x\neq y=0}^{2^n-1} \|x\rangle\langle y\|$ $+2^{-n}a^*b \|1\rangle\langle 0\| \otimes \sum_{x\neq y=0}^{2^n-1} \|y\rangle\langle x\|$ $\begin{cases} (1 \le L \le n):\ H_E = L \\ H_{SE} = (1-\delta_{L,n}) H(S_{class}) + L \end{cases}$
(5) $\frac{1}{2}(\|0_n\rangle\langle 0_n\| + \|1_{n-1}0\rangle\langle 1_{n-1}0\|)$ $H(S) = H(S_{class})\ \forall L$ ▲ – dotted curve	as in 1), with $\|0_{n-1}1\rangle \leftrightarrow \|1_{n-1}0\rangle$ $\begin{cases} (1 \le L \le n):\ H_E = 1 + \delta_{L,n} H(S_{class}) \\ H_{SE} = 1 + (1-\delta_{L,n}) H(S_{class}) \end{cases}$
$\|\Psi^{in}_E\rangle\langle\Psi^{in}_E\|$ (6) $\|\Psi^{in}_E\rangle = \frac{1}{\sqrt{2}}(\|0_n\rangle + \|1_n\rangle)$ ▼ – dotted curve	$\hat{\rho}^{in}_{S} \otimes \hat{\rho}^{in}_{E}$ $\begin{cases} H(S) = 0 < \forall L > 0 \\ H_E = H_{SE} = 1 - \delta_{L,n}\ (1 \le L \le n) \end{cases}$

for which one in general has $H(S, E_{L<n}) > 0$. Again, without loss of generality, let us set in (B.2) $L = n = 1$: w.r.t. (B.2) $\hat{\rho}^{out}_{E}(L = n = 1)$ remains the same as in (B.1), whereas $\hat{\rho}^{out}_{SE}(L = n = 1)$ from equation (B.2) leads $\forall\phi$ to non-zero eigenvalues

$$\lambda_1^{SE(L=n=1)} = |a|^2\ , \lambda_2^{SE(L=n=1)} = |b|^2\ .$$

Since $(c_1, c_2) > 0$ are parametrized by complementary transcendent functions of the ϕ-parameter, the only way to satisfy the MI-plateau condition between $H(S, E_L)$ and $H(E_L)$ is to demand $H(S, E_{L=n=1}) = H(E_{L=n=1})$, which can be achieved only if we choose

$$c_1^2 = c_2^2 = 1/2, \tag{B.3}$$

which leads to E-eigenstates $\{|s_1\rangle, |s_2\rangle\}$ of the CNOT-transformation $\widehat{u}_j^{(\phi=\pi/2)}$ from equation (6). Otherwise, $\forall(c_1 \neq c_2)$ one has $H(S, E_{L=n=1}) > H(E_{L=n=1})$. Thus, equation (B.3) shows that w.r.t. the S-pointer basis given by the standard computational basis $\{|\pi_i\rangle\} \equiv \{|0\rangle, |1\rangle\}$ solely the CNOT-transformation allows Quantum Darwinism to appear.

However, what happens if we generalize (6) to an open $k > 1$ qubit system S? Since there are only two eigenstates $\{|s_1\rangle, |s_2\rangle\}$ of $\widehat{u}_j^{(\phi=\pi/2)}$ in equations (7)–(8), the easiest way to generalize (B.2)–(B.3) to $k > 1$ S-qubits is according to

$$\hat{\rho}^{out}_{SE}(L) = \left(\sum_{i=0}^{2^{k-1}-1} |a_i|^2 |i\rangle\langle i|\right) \otimes \left|s_1^L\right\rangle\left\langle s_1^L\right| + \left(\sum_{j=2^{k-1}}^{2^k-1} |a_j|^2 |j\rangle\langle j|\right) \otimes \left|s_2^L\right\rangle\left\langle s_2^L\right|, \tag{B.4}$$

w.r.t. an arbitrary probability distribution of an open system S given by $1 > |a_i|^2 > 0$, $i \in \{0, \ldots, 2^k - 1\}$. However, the eigenvalues of equation (B.4),

$$\begin{aligned} &\hat{\rho}^{out}_{SE}(L) : \left\{\lambda_i^{SE} = |a_i|^2\right\}_{i=0}^{i=2^k-1} \\ &\Rightarrow (1-\delta_{k,1}) H(E_f) \le H(S, E_f) = H\left(S_{class}^{k\ge 1}\right)\ \forall L \\ &\hat{\rho}^{out}_{E}(L) : \lambda_1^E = \sum_{i=0}^{2^{k-1}-1} |a_i|^2\ ,\ \lambda_2^E = \sum_{j=2^{k-1}}^{2^k-1} |a_j|^2 \\ &\Rightarrow H(E_f) = -\sum_{i=1}^{2} \lambda_i^E \log_2 \lambda_i^E \le 1\ \forall L, \end{aligned} \tag{B.5}$$

indicate that QD appears for (B.4) if and only if $k = 1$, yielding

$$I(S:E_f)/H\left(S_{class}^{k\ge 1}\right) = H(E_f)/H\left(S_{class}^{k\ge 1}\right) = 1.$$

Accordingly, generalizing (B.1) with (B.3) as

$$\left|\Psi_{SE}^{out}(L)\right\rangle = \sum_{i=0}^{2^{k-1}-1} a_i \left|i\right\rangle \left|s_1^L\right\rangle + \sum_{j=2^{k-1}}^{2^k-1} a_j \left|j\right\rangle \left|s_2^L\right\rangle$$

$$\sum_{i=0}^{2^k-1} |a_i|^2 \stackrel{!}{=} 1,\ \hat{\rho}_{SE}^{out}(L) = \left|\Psi_{SE}^{out}(L)\right\rangle \left\langle\Psi_{SE}^{out}(L)\right|, \quad \text{(B.6)}$$

where $H(E_f) = -\sum_{i=1}^{2} \lambda_i^E \log_2 \lambda_i^E \leq 1 \forall L$ follows from (B.5), $H(S) = H(S_{class})$ and $H(S, E_f)$ behaves in a twofold way: (1) if $L = n \geq 1$, (B.6) is pure and we have the entropy relation $H(S, E_f) = 0 < H(E_f)$, yielding

$$I(S : E_f) = 2H(S_{class})$$

("quantum peak"); (2) For $1 \leq L < n$ (B.6) contains 2^{k-1} "diagonal S-subspaces", half of which are organized according to $\left|s_1^L\right\rangle \left\langle s_1^L\right|$, whereas the remaining 2^{k-1} "diagonal S-subspaces" of (B.6) are ordered according to $\left|s_2^L\right\rangle \left\langle s_2^L\right|$. This implies

$$I(S : E_f) = H(S_{class}) \ \forall (1 \leq L < n),$$

since $H(S, E_f) = H(E_f) = H\left(S_{class}^{k=1}\right)$, as in equation (B.5).

In equation (B.6) Quantum Darwinism does not appear for $k > 1$ and $1 \leq L \leq n$, since $\hat{\rho}_S^{out}$ of (B.6) has for $k \geq 1$ only two eigenvalues

$$\lambda_1^S = \sum_{i=0}^{2^{k-1}-1} |a_i|^2,\ \lambda_2^S = \sum_{j=2^{k-1}}^{2^k-1} |a_j|^2$$

(with $\lambda_1^S + \lambda_2^S \stackrel{!}{=} 1$), corresponding to eigenvalues of $k = 1$ system S. Thus: if we organize $\hat{\rho}_{SE}^{out}(L)$ according to (B.6), we could maximally store

$$1 \geq H(S_{class}) = -\lambda_1^S \log_2 \lambda_1^S - \lambda_2^S \log_2 \lambda_2^S > 0$$

of a $k = 1$ system S, even if one should insist on $k > 1$ (the PIP for $k = 1$ in Eq. (B.6) is given by Fig. 1), i.e. in equation (B.6) Quantum Darwinism appears only for $k = 1$.

Appendix C: Analytic reconstruction of attractor spaces

In this section we intend to sketch how one can reconstruct the maximal and minimal attractor spaces by utilizing the QR-decomposition method.

C.1 Maximal attractor space

The maximal attractor space and its basis states $\widehat{X}_{\lambda,i}$ of the random unitary evolution (7)–(9) w.r.t. a specific relevant eigenvalue λ follow as a solution to the eigenvalue equation (10) obtained by means of the QR-decomposition if we assume environment E to contain mutually non-interacting qubits. Since each directed edge of the ID in Figure 3 corresponds to an additional linear equation (constraint) in equation (10), the minimal number of constraints (and thus the maximal attractor space dimension $d_{n\geq k}^{\lambda}$) one could allow within the random unitary evolution model is given by the so called Koenig-IDs [11], in which only the S-qubits interact with E-qubits. In the following we will first determine $d_{n\geq k}^{\lambda}$.

C.1.1 Dimensionality

By implementing the QR-decomposition numerically one notices for $n \geq k$ that within the maximal attractor space there are only two subspaces with non-zero dimension d^{λ} associated with eigenvalues $\lambda = \pm 1$ of equation (10) [7–9]. From the numerically available data one can easily deduce for $n \geq k \geq 1$ that the following dimension formulas hold: for the eigenvalue $\lambda = 1$

$$d_n^{\lambda=1} = 4^n + 3 \cdot 2^n \left(2^k - 1\right) + \left(2^k - 1\right)\left(2^k - 2\right) + \delta_{n=k,1}, \quad \text{(C.1)}$$

for the eigenvalue $\lambda = -1$

$$d_n^{\lambda=-1} = 3 \cdot 2^n + 3 \cdot 2^k - 6 - 5 \cdot \delta_{n=k,1}. \quad \text{(C.2)}$$

Equations (C.1)–(C.2) can be easily proven by induction. Furthermore, one also sees from numerical data that for $k > n$ one has $d_{n<k}^{\lambda} = d_{n\leftrightarrow k}^{\lambda} \forall \lambda$, i.e. $d_{n<k}^{\lambda}$ follows from $d_{n'=k\geq k'=n}^{\lambda}$ after interchanging k with n in equations (C.1)–(C.2).

C.1.2 State structure

Implementing the QR-decomposition (see Ref. [12]) for IDs with mutually non-interacting E-qubits and using the environmental $\widehat{u}_j^{(\phi)}$-symmetry states $\{|s_{c_1}^L\rangle, |s_{c_2}^L\rangle\}$ from equations (B.1)–(B.2) to classify the solutions (attractor states) $\widehat{X}_{\lambda,i}$ of equation (10) one obtains $\forall (n \geq k \geq 1)$ the following two attractor subspaces associated with the two relevant eigenvalues $\lambda \in \{1, -1\}$:

$$\left.\begin{array}{c} |0_k\rangle\langle x| \otimes |y\rangle\langle s_{c_1}^n|,\ |x\rangle\langle 0_k| \otimes |s_{c_1}^n\rangle\langle y| \\ |0_k\rangle\langle 0_k| \otimes |y\rangle\langle z| \\ |x\rangle\langle x| \bigotimes_{i=1}^{n} A_{\gamma_i},\ |x\rangle\langle w| \otimes |s_{c_1}^n\rangle\langle s_{c_1}^n| \end{array}\right\} \lambda = 1, \quad \text{(C.3)}$$

with

$$|\chi_k\rangle = |\chi\rangle^{\otimes k},\ (\chi, \gamma_i) \in \{0, 1\}$$
$$(x, w) \in \left\{0, \ldots, 2^k - 1\right\},\ (y, z) \in \{0, \ldots, 2^n - 1\}$$
$$(x \neq w) \neq 0_k,\ A_0 = |s_{c_1}\rangle\langle s_{c_1}|,\ A_1 = \hat{I} - |s_{c_1}\rangle\langle s_{c_1}|$$

and

$$\left.\begin{array}{c} |0_k\rangle\langle 1_k| \otimes |y\rangle\langle s^n_{c_2}|,\ |1_k\rangle\langle 0_k| \otimes |s^n_{c_2}\rangle\langle y| \\ |1_k\rangle\langle 1_k| \overset{n}{\underset{i=1}{\otimes}} B_{\gamma_i},\ |x\rangle\langle x| \otimes |s^n_{c_2}\rangle\langle s^n_{c_2}| \\ |x\rangle\langle 1_k| \otimes |s^n_{c_1}\rangle\langle s^n_{c_2}|,\ |1_k\rangle\langle x| \otimes |s^n_{c_2}\rangle\langle s^n_{c_1}| \end{array}\right\} \lambda = -1, \quad \text{(C.4)}$$

with

$$x \neq (0_k,\, 1_k),\ B_0 = \left(\sqrt{2}\right)^{-1} (|0\rangle\langle 1| - |1\rangle\langle 0|)$$
$$B_1 = \left(\sqrt{2}\right)^{-1} [-\sin\phi|0\rangle\langle 0| + \sin\phi|1\rangle\langle 1| + \cos\phi|0\rangle\langle 1| + \cos\phi|1\rangle\langle 0|]\,.$$

Equations (C.3)–(C.4) are in accord with equations (C.1)–(C.2) and contain orthonormalized attractor states $\widehat{X}_{\lambda,i}$, with

$$\left\langle \widehat{X}_{\lambda,i},\, \widehat{X}_{\lambda',i'} \right\rangle := \delta_{\lambda,\,\lambda'}\delta_{i,\,i'},$$

given by the Hilbert-Schmidt scalar product

$$\left\langle \widehat{X}_{\lambda,i},\, \widehat{X}_{\lambda',i'} \right\rangle := \mathrm{Tr}\left[\widehat{X}_{\lambda,i}\left(\widehat{X}_{\lambda',i'}\right)^{\dagger}\right].$$

C.2 Minimal attractor space

Now we turn our attention to environments E whose all n qubits are allowed to mutually interact with each other, as depicted by the ID in Figure 3 and already studied in references [7–9].

C.2.1 Dimensionality

From [7–9] we know that E enclosing mutually via $\widehat{u}^{(\phi)}_j$ interacting n qubits (with $n \geq k \geq 1$) leads to the the most constrained (strongly connected) ID with an attractor subspace associated with the eigenvalue $\lambda = 1$ of equation (10) of minimal dimension

$$d_n^{\lambda=1,min} = 4^k + 3\cdot 2^k + 1, \quad \text{(C.5)}$$

whereas the dimensionality of the $\lambda = -1$ attractor subspace satisfies

$$d_n^{\lambda=-1,min} = \begin{cases} 1 \text{ if } n = k = 1 \\ 0, \text{ otherwise.} \end{cases} \quad \text{(C.6)}$$

Since Quantum Darwinism involves environments E with $n \gg 1$ qubits, we may conclude that within the minimal attractor space only the $\lambda = 1$ subspace contributes to the evolution of $\hat{\rho}^{in}_{SE}$.

C.2.2 State structure

From [7–9] we know that (C.5) corresponds to the following structure of the linear independent (however not yet orthonormalized) $\widehat{X}_{\lambda=1,i}$-states

$$|x\rangle\langle x| \otimes \hat{\mathrm{I}}_n,\ |0_k\rangle\langle x| \otimes |0_n\rangle\left\langle s^n_{c_1}\right|,\ |x\rangle\langle 0_k| \otimes \left|s^n_{c_1}\right\rangle\langle 0_n|$$
$$|x\rangle\langle y| \otimes \left|s^n_{c_1}\right\rangle\left\langle s^n_{c_1}\right|,\ |0_k\rangle\langle 0_k| \otimes |0_n\rangle\langle 0_n|\,, \quad \text{(C.7)}$$

whereas (C.6) corresponds for $k = n = 1$ to the only non-zero orthonormalized $\widehat{X}_{\lambda=-1,i}$-state

$$\hat{X}^{n=k=1}_{\lambda=-1,\,i=1} = \frac{1}{\sqrt{6}}\left(|01\rangle\langle 11| - |10\rangle\langle 11| - |11\rangle\langle 01| + |11\rangle\langle 10| - |01\rangle\langle 10| + |10\rangle\langle 01|\right), \quad \text{(C.8)}$$

with

$$(x,\, y) \in \{0,\, \ldots,\, 2^k - 1\},\ \mathrm{Tr}_E\left[\hat{\mathrm{I}}_n\right] = 2^n,\ \hat{\mathrm{I}}_n = \hat{\mathrm{I}}_1^{\otimes n}$$

and $\{|s^L_{c_1}\rangle, |s^L_{c_2}\rangle\}$ from equations (B.1)–(B.2). However, equation (C.8) does not contribute to the evolution of $\hat{\rho}^{in}_{SE}$ from the point of view of Quantum Darwinism, which necessitates us to start with $\hat{\rho}^{in}_{SE}$ enclosing environments E with $n \gg k \geq 1$ qubits.

Appendix D: Output states $\hat{\rho}^{\mathbf{out}}_{\mathbf{SE_L}}$ of the random unitary evolution used in Section 3

In this appendix we list the output states $\hat{\rho}^{out}_{SE_L}$ of the random unitary evolution used in Section 3.

D.1 Output states $\hat{\rho}^{\mathbf{out}}_{\mathbf{SE_L}}$ of the random unitary evolution for the maximal attractor space

In this appendix we list the output states $\hat{\rho}^{out}_{SE_L}$ of the random unitary evolution used in Section 3 of the main text when discussing Quantum Darwinism from the point of view of the maximal attractor space.

(I) Input: $\hat{\rho}^{in}_{SE} = \left|\Psi^{in}_S\right\rangle\left\langle\Psi^{in}_S\right| \otimes \hat{\rho}^{in}_E$, $\left|\Psi^{in}_S\right\rangle = \sum_{m=0}^{2^k-1} a_m |m\rangle$, $\hat{\rho}^{in}_E = \left|z^{L=n}\right\rangle\left\langle z^{L=n}\right|$, $\widehat{u}^{(\phi=\pi/2)}_j$-evolution

see equation (D.1) next page

where $z^{L=n} \in \{0,\, \ldots,\, 2^n - 1\}$, $\{|s_1\rangle, |s_2\rangle\}$ as in (6), $\langle s_1|\,\xi\rangle = 2^{-1/2}$, $\langle s_2|\,\xi\rangle = (-1)^{\xi}\,2^{-1/2}$ for $\xi \in \{0,\, 1\}$,

$$|\Psi'\rangle = a_0\,|0\rangle \otimes |z^n\rangle + \sum_{m=1}^{2^k-1} a_m 2^{-n/2}\,|m\rangle \otimes |s^n_1\rangle\,,$$
$$\hat{B}^{\pi/2}_1 = \left(\sqrt{2}\right)^{-1}[|1\rangle\langle 1| - |0\rangle\langle 0|]\,,$$

and M is the number of $|1\rangle$-one qubit states in $\left|z^{L=n}\right\rangle$.

$$\hat{\rho}_{SE}^{out} = \left|\Psi'\right\rangle\left\langle\Psi'\right| + 2^{-n}\sum_{m=1}^{2^k-1}\left|a_m\right|^2\left|m\right\rangle\left\langle m\right|\otimes\left(\widehat{I}_n - \left|s_1^n\right\rangle\left\langle s_1^n\right|\right)$$
$$+ (-1)^N\cdot\left\{2^{-n/2}(-1)^M\left[a_0 a_{2^k-1}^*\left|0\right\rangle\left\langle 2^k-1\right|\otimes\left|z^n\right\rangle\left\langle s_2^n\right| + a_{2^k-1}a_0^*\left|2^k-1\right\rangle\left\langle 0\right|\otimes\left|s_2^n\right\rangle\left\langle z^n\right|\right]\right.$$
$$+ 2^{-n}\sum_{m=1}^{2^k-2}\left|a_m\right|^2\left|m\right\rangle\left\langle m\right|\otimes\left|s_2^n\right\rangle\left\langle s_2^n\right| + (-1)^n\cdot 2^{-n/2}\left|a_{2^k-1}\right|^2\left|2^k-1\right\rangle\left\langle 2^k-1\right|\bigotimes_{i=1}^{n}\hat{B}_1^{\pi/2}$$
$$\left.+2^{-n}\sum_{m=1}^{2^k-2}a_m a_{2^k-1}^*\left|m\right\rangle\left\langle 2^k-1\right|\otimes\left|s_1^n\right\rangle\left\langle s_2^n\right| + 2^{-n}\sum_{m=1}^{2^k-2}a_{2^k-1}a_m^*\left|2^k-1\right\rangle\left\langle m\right|\otimes\left|s_2^n\right\rangle\left\langle s_1^n\right|\right\}, \tag{D.1}$$

$$\hat{\rho}_{SE}^{out} = \left|a_0\right|^2\left|0\right\rangle\left\langle 0\right|\otimes\hat{\rho}_E^{in} + \left|a_1\right|^2\left|1\right\rangle\left\langle 1\right|\otimes 2^{-n}\hat{I}_n$$
$$+ 2^{-n/2-1}\cdot\left(a_0 a_1^*\left|0\right\rangle\left\langle 1\right|\otimes\left[\left|0_n\right\rangle\left\langle s_1^n\right| + \left|1_n\right\rangle\left\langle s_1^n\right|\right] + a_1 a_0^*\left|1\right\rangle\left\langle 0\right|\otimes\left[\left|s_1^n\right\rangle\left\langle 0_n\right| + \left|s_1^n\right\rangle\left\langle 1_n\right|\right]\right)$$
$$+ (-1)^N\left\{2^{-n/2-1}\left(a_0 a_1^*\left|0\right\rangle\left\langle 1\right|\otimes\left[\left|0_n\right\rangle\left\langle s_2^n\right| + (-1)^n\left|1_n\right\rangle\left\langle s_2^n\right|\right]\right.\right.$$
$$\left.\left.+ a_1 a_0^*\left|1\right\rangle\left\langle 0\right|\otimes\left[\left|s_2^n\right\rangle\left\langle 0_n\right| + (-1)^n\left|s_2^n\right\rangle\left\langle 1_n\right|\right]\right) + 2^{-1}\left|a_1\right|^2\left|1\right\rangle\left\langle 1\right|2^{-n/2}\left(1+(-1)^n\right)\bigotimes_{i=1}^{n}\hat{B}_1^{\pi/2}\right\} \tag{D.2}$$

(II) Input: $\hat{\rho}_{SE}^{in} = \left|\Psi_S^{in}\right\rangle\left\langle\Psi_S^{in}\right|\otimes\hat{\rho}_E^{in}$, $\left|\Psi_S^{in}\right\rangle = \sum_{m=0}^{2^{k=1}-1}a_m\left|m\right\rangle$, $\hat{\rho}_E^{in} = 2^{-1}\left(\left|0_n\right\rangle\left\langle 0_n\right| + \left|1_n\right\rangle\left\langle 1_n\right|\right)$, $\widehat{u}_j^{(\phi=\pi/2)}$-evolution

see equation (D.2) above.

(III) Input: $\hat{\rho}_{SE}^{in} = \left|\Psi_S^{in}\right\rangle\left\langle\Psi_S^{in}\right|\otimes\hat{\rho}_E^{in}$, $\left|\Psi_S^{in}\right\rangle = \sum_{m=0}^{2^{k=1}-1}a_m\left|m\right\rangle$, $\hat{\rho}_E^{in} = 2^{-n}\hat{I}_n$, $\widehat{u}_j^{(\phi=\pi/2)}$-evolution

$$\hat{\rho}_{SE}^{out}(L=n) = \left(\left|a_0\right|^2\left|0\right\rangle\left\langle 0\right| + \left|a_1\right|^2\left|1\right\rangle\left\langle 1\right|\right)\otimes 2^{-n}\hat{I}_n$$
$$+ \left(a_0 a_1^*\left|0\right\rangle\left\langle 1\right| + a_1 a_0^*\left|1\right\rangle\left\langle 0\right|\right)\otimes 2^{-n}$$
$$\times\left(\left|s_1^{L=n}\right\rangle\left\langle s_1^{L=n}\right| + (-1)^N\left|s_2^{L=n}\right\rangle\left\langle s_2^{L=n}\right|\right). \tag{D.3}$$

(IV) Input: $\hat{\rho}_{SE}^{in} = \left|\Psi_S^{in}\right\rangle\left\langle\Psi_S^{in}\right|\otimes\hat{\rho}_E^{in}$, $\left|\Psi_S^{in}\right\rangle = \sum_{m=0}^{2^{k=1}-1}a_m\left|m\right\rangle$, $\hat{\rho}_E^{in} = 2^{-1}\left(\left|0_n\right\rangle\left\langle 0_n\right| + \left|10_{n-1}\right\rangle\left\langle 10_{n-1}\right|\right)$, $\widehat{u}_j^{(\phi=\pi/2)}$-evolution

$\hat{\rho}_{SE}^{out}(L=n)$ emerges from equation (D.2) by applying the following substitutions:

$$\left|1_n\right\rangle \leftrightarrow \left|10_{n-1}\right\rangle, (-1)^n\left(\left|1_n\right\rangle\left\langle s_2^L\right| + h.c.\right)$$
$$\leftrightarrow (-1)^1\left(\left|10_{n-1}\right\rangle\left\langle s_2^L\right| + h.c\right)$$
$$\left(1+(-1)^n\right)\bigotimes_{i=1}^{n}\hat{B}_1^{\pi/2}\cdot\delta_{L,n} \leftrightarrow (-1)^{n-1}\bigotimes_{i=1}^{n}\hat{B}_1^{\pi/2}\cdot\delta_{L,n}. \tag{D.4}$$

(V) Input: $\left|\Psi_{SE}^{in}\right\rangle = a\left|0_{k=1}\right\rangle\otimes\left|s_1^{L=n}\right\rangle + b\left|1_{k=1}\right\rangle\otimes\left|s_2^{L=n}\right\rangle$, $\widehat{u}_j^{(\phi=\pi/2)}$-evolution

$$\left|\Psi_{SE_{L=n}}^{out}\right\rangle = a\left|0\right\rangle\otimes\left|s_1^n\right\rangle + (-1)^N b\left|1\right\rangle\otimes\left|s_2^n\right\rangle. \tag{D.5}$$

D.2 Output states $\hat{\rho}_{SE}^{out}$ of the random unitary evolution for the minimal attractor space

In this appendix we list the output states $\hat{\rho}_{SE_L}^{out}$ of the random unitary evolution used in Section 3 of the main text when discussing Quantum Darwinism from the point of view of the minimal $\lambda = 1$ attractor subspace.

(I) Input: $\hat{\rho}_{SE}^{in} = \left|\Psi_S^{in}\right\rangle\left\langle\Psi_S^{in}\right|\otimes\hat{\rho}_E^{in}$, $\left|\Psi_S^{in}\right\rangle = \sum_{m=0}^{2^k-1}a_m\left|m\right\rangle$, $\hat{\rho}_E^{in} = \left|0_n\right\rangle\left\langle 0_n\right|$, $\widehat{u}_j^{(\phi=\pi/2)}$-evolution

$$\widehat{\rho}_{SE}^{out} = \left|\Psi'\right\rangle\left\langle\Psi'\right| + 2^{-n}\sum_{y=1}^{2^k-1}\left|a_y\right|^2\left|y\right\rangle\left\langle y\right|\otimes\left(\widehat{I}_n - \left|s_1^n\right\rangle\left\langle s_1^n\right|\right), \tag{D.6}$$

where

$$\left|\Psi'\right\rangle = a_0\left|0\right\rangle\otimes\left|0_n\right\rangle + \sum_{y=1}^{2^k-1}a_y 2^{-n/2}\left|y\right\rangle\otimes\left|s_1^n\right\rangle.$$

(II) Input: $\hat{\rho}_{SE}^{in} = \left|\Psi_S^{in}\right\rangle\left\langle\Psi_S^{in}\right| \otimes \hat{\rho}_E^{in}$, $\left|\Psi_S^{in}\right\rangle = \sum_{m=0}^{2^k-1} a_m \left|m\right\rangle$, $\hat{\rho}_E^{in} = \left|1_n\right\rangle\left\langle 1_n\right|$, $\widehat{u}_j^{(\phi=\pi/2)}$-evolution

$$\begin{aligned}\widehat{\rho}_{SE}^{out} &= \left|a_0\right|^2 2^{-n}\left(1-2^{-n}\right)^{-1}\left|0\right\rangle\left\langle 0\right| \\ &\otimes\left(\widehat{I}_n 2^{-n} - \left|0_n\right\rangle\left\langle 0_n\right|\right) + 2^{-n}\sum_{y=0}^{2^k-1}\left|a_y\right|^2\left|y\right\rangle\left\langle y\right| \otimes \widehat{I}_n \\ &- 2^{-3n/2}\left(1-2^{-n}\right)^{-1}\sum_{y=1}^{2^k-1}\Big\{a_0 a_y^*\left|0\right\rangle\left\langle y\right| \otimes \left|0_n\right\rangle \\ &\times\left\langle s_1^n\right| + a_y a_0^*\left|y\right\rangle\left\langle 0\right| \otimes \left|s_1^n\right\rangle\left\langle 0_n\right|\Big\} \\ &+ 2^{-n}\sum_{(x\neq y)=1}^{2^k-1}\Big\{\left(1-2^{-n}\right)^{-1} a_0 a_y^*\left|0\right\rangle\left\langle y\right| \\ &+ \left(1-2^{-n}\right)^{-1} a_y a_0^*\left|y\right\rangle\left\langle 0\right| + a_y a_x^*\left|y\right\rangle\left\langle x\right|\Big\} \\ &\otimes\left|s_1^n\right\rangle\left\langle s_1^n\right|. \end{aligned} \tag{D.7}$$

(III) Input: $\hat{\rho}_{SE}^{in} = \left|\Psi_S^{in}\right\rangle\left\langle\Psi_S^{in}\right| \otimes \hat{\rho}_E^{in}$, $\left|\Psi_S^{in}\right\rangle = \sum_{m=0}^{2^{k=1}-1} a_m \left|m\right\rangle$, $\hat{\rho}_E^{in} = 2^{-1}\left(\left|0_n\right\rangle\left\langle 0_n\right| + \left|1_n\right\rangle\left\langle 1_n\right|\right)$, $\widehat{u}_j^{(\phi=\pi/2)}$-evolution

$$\begin{aligned}\widehat{\rho}_{SE}^{out} &= \left|a_0\right|^2\left|0\right\rangle\left\langle 0\right|\left(1-2^{-n}\right)^{-1} \\ &\otimes\Big\{\widehat{I}_n 2^{-n-1} + \left|0_n\right\rangle\left\langle 0_n\right|\left(1-2^{1-n}\right)^{-1} \\ &\times\left(\frac{1}{2} - 2^{1-n} + 2^{1-2n}\right)\Big\} + \left|a_1\right|^2\left|1\right\rangle\left\langle 1\right| \otimes 2^{-n}\widehat{I}_n \\ &+ a_0 a_1^* 2^{-1}\left(1-2^{1-n}\right)^{-1}\left|0\right\rangle\left\langle 1\right| \\ &\otimes\Big\{\left|0_n\right\rangle\left\langle s_1^n\right| 2^{-n/2}\left(1-2^{1-n}\right) + 2^{-n}\left|s_1^n\right\rangle\left\langle s_1^n\right|\Big\} \\ &+ a_1 a_0^* 2^{-1}\left(1-2^{1-n}\right)^{-1}\left|1\right\rangle\left\langle 0\right| \\ &\otimes\Big\{\left|s_1^n\right\rangle\left\langle 0_n\right| 2^{-n/2}\left(1-2^{1-n}\right) + 2^{-n}\left|s_1^n\right\rangle\left\langle s_1^n\right|\Big\}. \end{aligned} \tag{D.8}$$

(IV) Input: $\hat{\rho}_{SE}^{in} = \left|\Psi_S^{in}\right\rangle\left\langle\Psi_S^{in}\right| \otimes \hat{\rho}_E^{in}$, $\left|\Psi_S^{in}\right\rangle = \sum_{m=0}^{2^k-1} a_m \left|m\right\rangle$, $\hat{\rho}_E^{in} = 2^{-n}\hat{I}_n$, $\widehat{u}_j^{(\phi=\pi/2)}$-evolution

$$\begin{aligned}\widehat{\rho}_{SE}^{out} &= \sum_{x=0}^{2^k-1}\left|a_x\right|^2\left|x\right\rangle\left\langle x\right| \otimes \hat{\rho}_E^{in} \\ &+ 2^{-n}\sum_{(x\neq y)=0}^{2^k-1} a_x a_y^*\left|x\right\rangle\left\langle y\right| \otimes \left|s_1^n\right\rangle\left\langle s_1^n\right|. \end{aligned} \tag{D.9}$$

(V) Input: $\left|\Psi_{SE}^{in}\right\rangle = a\left|0_{k=1}\right\rangle \otimes \left|s_1^L\right\rangle + b\left|1_{k=1}\right\rangle \otimes \left|s_2^L\right\rangle$, $\widehat{u}_j^{(\phi=\pi/2)}$-evolution

$$\begin{aligned}\widehat{\rho}_{SE}^{out} &= \left|a_0\right|^2\left|0\right\rangle\left\langle 0\right| \otimes \left|s_1^n\right\rangle\left\langle s_1^n\right| + \left|a_1\right|^2\left(2^n-1\right)^{-1}\left|1\right\rangle\left\langle 1\right| \\ &\otimes\left(\widehat{I}_n - \left|s_1^n\right\rangle\left\langle s_1^n\right|\right). \end{aligned} \tag{D.10}$$

References

1. E. Joos et al., *Decoherence and the Appearence of a Classical World in Quantum Theory* (Springer, 2003)
2. F.G.S.L. Brandão, M. Piani, P. Horodecki, *Quantum Darwinism is generic*, Nat. Com. **6**, 7908 (2015)
3. W.H. Zurek, Nat. Phys. **5**, 181 (2009)
4. R. Blume-Kohout, W.H. Zurek, Found. Phys. **35**, 1857 (2005)
5. W.H. Zurek, Philos. Trans. R. Soc. Lond. Ser. A **356**, 1793 (1998)
6. W.H. Zurek, Phys. Rev. D **26**, 1862 (1982)
7. J. Novotný, G. Alber, I. Jex, New J. Phys. **13**, 053052 (2011)
8. J. Novotný, G. Alber, I. Jex, Phys. Rev. Lett. **107**, 090501 (2011)
9. J. Novotný, G. Alber, I. Jex, J. Phys. A **45**, 485301 (2012)
10. M. Berta, J.M. Rennes, M.M. Wilde, IEEE **60**, 7987 (2014)
11. R. Brualdi, D. Cvetkovic, *A Combinatorial Approach to Matrix Theory* (Taylor and Francis, 2010)
12. D. Serre, *Matrices – Theory and Applications*, 2nd edn. (Springer GTM, 2010)